A PARAMETRIC STUDY OF THE EFFECTS OF ε AND $\bar{k}$ ON THE POISSON

BOLTZMANN EQUATION FOR ONE AND TWO SPHERICAL PARTICLES

USING A BOUNDARY INTEGRAL EQUATION METHOD

by

OUMAMA H LINGAMFELTER

Presented to the Faculty of the Graduate School of

The University of Texas at Arlington in Partial Fulfillment

of the Requirements

for the Degree of

MASTER OF SCIENCE IN MECHANICAL ENGINEERING

THE UNIVERSITY OF TEXAS AT ARLINGTON

May 2015

Acknowledgements

I would first like to sincerely thank Dr. Bo Yang for his help, guidance and invaluable input during this process. He is truly a great mentor. I appreciate his unwavering support during these last couple of years. He inspired my intellectual curiosity and encouraged me to explore my ideas on this topic. His open door policy is one of the many examples of his great leadership skills.

I would also like to extend a big thank you to my committee members, Dr. Kent Lawrence and Dr. Ratan Kumar, for taking the time out of their busy schedule to advise me. I would also like to particularly thank Dr. Lawrence for being such an outstanding professor and mentor.

Next, I would like to extend my deepest gratitude and appreciation to my loving husband Max, whose patience and support were unparalleled during this process. I deeply appreciate his help and understanding during the long hours spent on campus.

I would also like to thank my mother, who has been a wonderful model for me growing up. She is a wonderful example of a strong, intelligent and accomplished person.

Finally, I would like to extend a special thank you to Debbie, Lanie, and Flora for always knowing the right thing to say and always putting a smile on my face.

May 4, 2015

Abstract

A PARAMETRIC STUDY OF THE EFFECTS OF ε AND $\bar{k}$ ON THE POISSON

BOLTZMANN EQUATION FOR ONE AND TWO SPHERICAL PARTICLES

USING A BOUNDARY INTEGRAL METHOD

Oumama H Lingamfelter, M.S.

The University of Texas at Arlington, 2015

Supervising Professor: Bo Yang

Many biomolecules, such as DNA, exhibit properties that are dependent on their electrostatic interaction with an electrolytic solution. Both explicit atomistic and implicit continuum models have been developed to solve the electrostatic problem. The implicit models are based on the Poisson-Boltzmann (PB) equation, whose lower computational cost makes them favored for bio-molecular applications, particularly as the molecule size increases. Among the implicit models, a boundary integral equation (BIE) method involving only numerical treatment on a surface in turn is more efficient than domain-based finite element and finite difference methods. This is especially so in the present case where the electric field varies exponentially requiring specially designed adaptive mesh in the domain-based methods. However, the BIE method is only applicable to linearized PB equation whose fundamental solution is available in an analytical

iv

form. When coupled with the linear interfacial continuity condition, it is only valid for low-voltage surfaces. In the present work, a nonlinear interfacial continuity condition is introduced by relating the asymptotes of the nonlinear and the linear PB equations at a surface. Equipped with it, the BIE method can be applied to efficiently and accurately solve the PB problems with high voltage surfaces. Its validity and capability are demonstrated with benchmark examples with one and two spherical particles. In particular, the particle solvation energy is calculated. In the case of two particles, the particle interaction energy is also calculated. The effects of the Debye length of the electrolytic solution and the dielectric mismatch between a particle and the electrolytic solution are examined in detail. A comparison of the linear and the nonlinear PB solutions shows their great difference for highly charged particles, not only in magnitude but also sometimes in variation trend with charge magnitude.

Table of Contents

List of Illustrations

List of Tables

Chapter 1

Introduction

The Poisson Boltzmann equation (PBE) is a second order partial

difference equation that describes the electrostatic interaction of a molecule and

the ionic solution space. Many biomolecules, such as DNA, have properties that

are dependent on these interactions. The ionic distribution and charge interaction

of the system is important in many domains. Examples include protein folding

and protein binding. Protein folding, an area of intense interest in scientific

research, describes the tertiary structure of the amino acids. It determines the

function and efficiency of the protein.
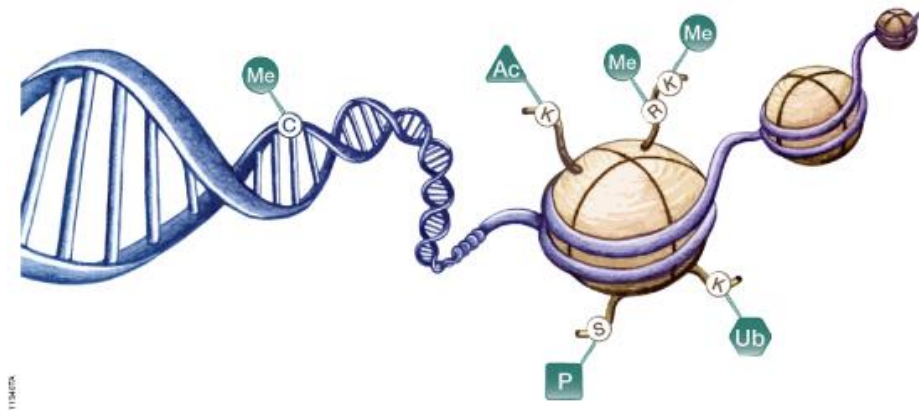
Figure 1: DNA Methylation, an Example of Protein Binding Involved in Gene

Expression and Epigenetics. (1)

Protein-protein binding governs intercellular transport. The coagulation cascade, hormone synthesis, cell metabolism and intercellular transport are all examples of protein interaction regulated by protein binding. While the PBE is germane to bio-molecular systems, similar applications can be found in electrochemistry, biophysics, biochemistry, and many other fields.
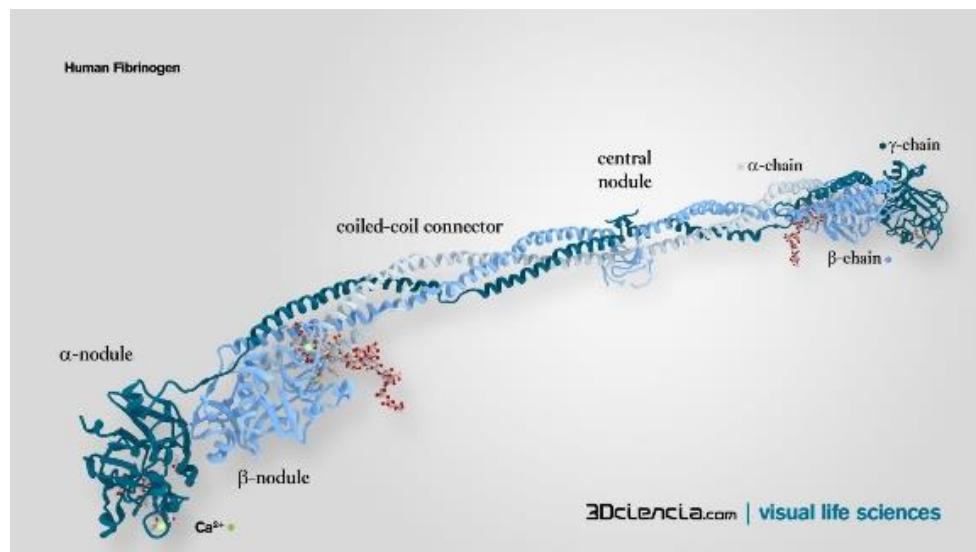
Figure 2: An Example of a Complicated Tertiary Protein Structure, Fibrinogen, Involved in Hemostasis. (2)
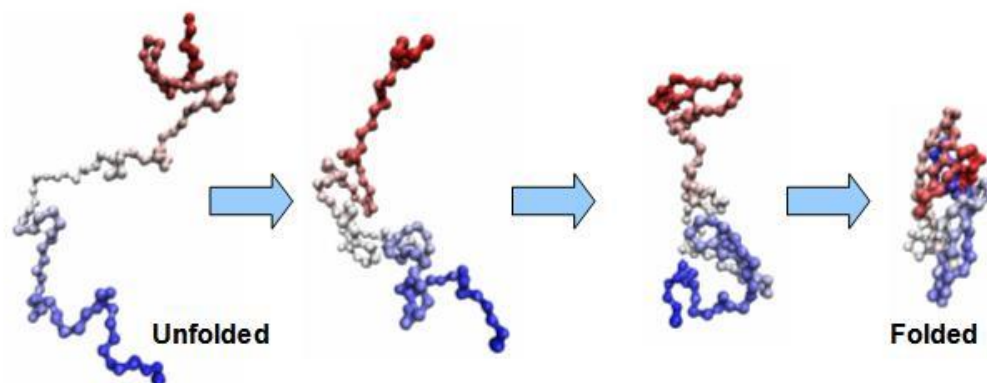
Figure 3: The Folding Process of a Protein (3)

While both explicit and implicit models have been developed to study the above interactions, the implicit models' lower computational cost makes them a more attractive solution for bio-molecular applications, particularly as the molecule size increases. The explicit model requires both the solvent and the solute to be examined at the atomic level whereas the implicit model allows for the approximation of the atomic details of the solvent. While some of the detail is lost when using the implicit model, other important properties can be reasonably well measured, such as the solvation energy. Although one of the most common approaches to solving the implicit model is by means of the PBE, its accuracy depends heavily on the simplicity of the geometry and the size of the system. The complexity of the PBE requires the use of numerical methods. Currently, the finite element method (FEM), finite difference method (FDM) and boundary element method (BEM) are the prevalent methods. Each of these approaches have inherent positives and limitations as discussed below.

1.1 Finite Difference Method

The finite difference method discretizes the domain and approximates a solution to the PBE using one of the finite difference equations. In the bio-molecular field, the PBE has been mainly solved using this approach. This is due to the low computational cost of generating and refining the mesh required. APBS, currently the most common solver, uses a finite difference approach. The properties that are location-dependent, such as density and potential, are represented on a lattice. The finite difference equations shown below are then used to approximate those properties in a different location (4).

There are two means of improving the accuracy of FDM. One involves using a coarse mesh in the solvent region and a refined mesh near the molecular surface. The other utilizes a coarse mesh to obtain the ionic distribution of the system. Boundary conditions are then interpolated and applied to a finer mesh (17).

There are some limitations to using FDM. FDM requires a boundary conforming mesh and uses a finite grid which requires an approximation for the outer boundary. Moreover, FDM solves the PBE for the entire 3-D domain resulting in a large number of unknowns. The use of a grid in FDM leads to a lower accuracy when compared to the solution of BEM as BEM solves the PBE for every point in the surface (9). Finally, the movement of the biomolecules during the transport process makes the meshing particularly burdensome.

$f_{i,j+1}$
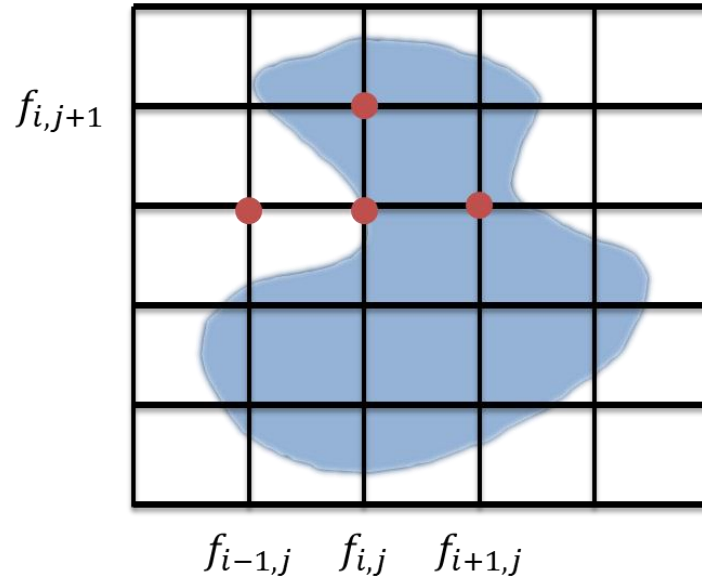
$f_{i-1,j}$ $f_{i,j}$ $f_{i+1,j}$

Figure 4: Approximation of the Solution Using Finite Difference Method

Equations 1,2,3: Finite Difference Equations: Central Difference, Backward Difference and Forward Difference for a two Dimensional Mesh

$$f_{i,j} = \frac{f_{i+1,j} - f_{i-1,j}}{2\Delta x} \tag{1}$$

$$f_{i+1,j} = \frac{f_{i,j} - f_{i-1,j}}{\Delta x} \tag{2}$$

$$f_{i-1,j} = \frac{f_{i+1,j} - f_{i,j}}{\Delta x} \tag{3}$$

1.2 Finite Element Method

The finite element method discretizes the domain into multiple "elements" with connecting nodes and solves the PBE for each of these elements. FEM

allows for easier mesh refinement and faster convergence. It also provides more

accurate results to non-linear equations. However, this comes at a high

computational cost.
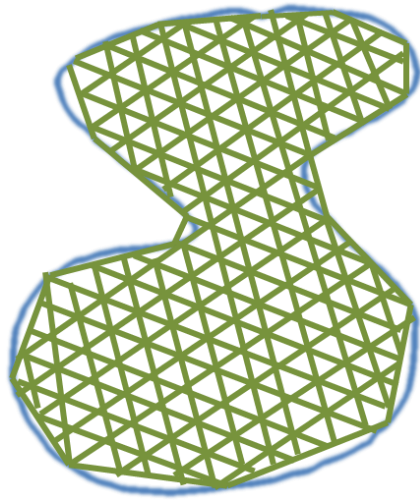
Figure 5: Element Discretization of a Molecule Using Finite Element Method

1.3 Boundary Element Method

Boundary element method, also known as boundary integral method,

involves formulating partial differential equations in boundary integral form. A

discretized integral equation that is mathematically equivalent to the PDE is

defined using the boundary of the domain and a correlation integral. The

correlation integral relates the solution at the boundary to the points within the

domain. Since only linear PDE's can be described using this method, the

boundary element method is not as widely used as the finite difference and finite

element methods. When the boundary element method can be applied, it usually can be done with greater ease and less computational cost. While in FEM or FDM the entire domain must be subdivided, only the boundary of the system requires the discretization of the PDE. By utilizing the BEM method, the overall dimension of the problem can be reduced by 1. In two dimensional domains, straight lines may be used. In three dimensional and axisymmetric problems, planar triangles and truncated conical panels can be used respectively (Figure 5).
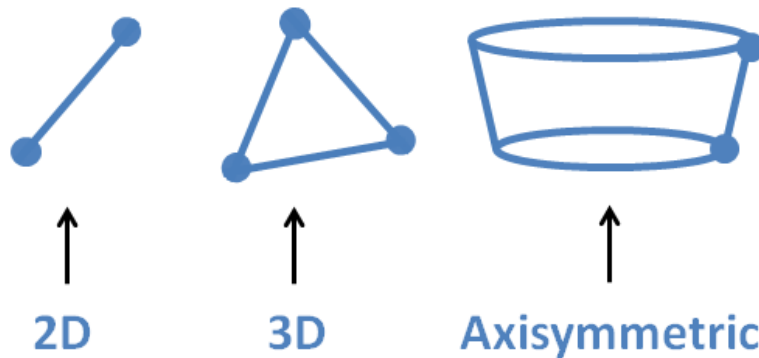
Figure 6: Boundary Panel Approximations in Boundary Element Method.

An example of the benefit of BEM in biomolecules is shown in figure 6. Using only straight lines, the two dimensional domain can be described by a series of similar panels, providing a way of approximating the boundary with a series of numbered 1-D data structures. Although the resulting stiffness matrix is quite dense, it can be reduced using a fast multipole method. While this leads to a

loss of accuracy, it is still more advantageous than the domain based approaches

(5). One drawback to using the boundary integral method however, is its

dependence on linear equations. In order to satisfy this requirement, the Poisson

Boltzmann Equation is linearized in chapter 2. This linearization limits the use of

the boundary element method to problems of low zeta potential, where the

solutions of the Poisson Boltzmann equation and the linearized Poisson

Boltzmann equation only differ slightly.
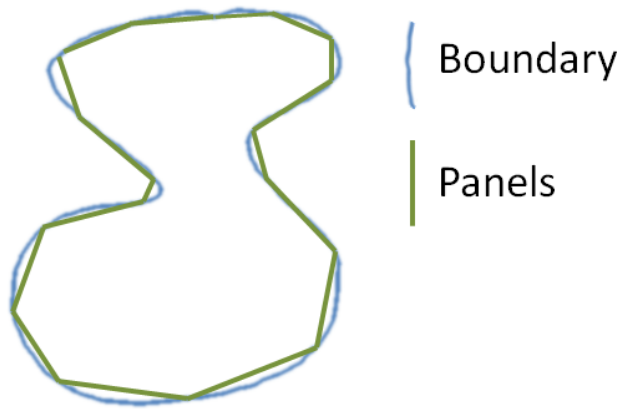
Figure 7: Two Dimensional Domain as Described by a Series of Straight Line

Panels, an Example of Applied BEM.

In addition to its use of a lower dimensionality, BEM offers several

additional advantages. Surface and far field boundary conditions are inherently

implemented in the BEM. Moreover, BEM solves the equation for a 2-D surface

resulting in a fewer number of unknowns when compared to FDM. Their lack of grid structure allows BEM to solve the PDE at every point in the surface, resulting in a superior solution to multimolecular dynamic simulations.

1.4 Recent advances in electrostatic modeling

Geng and Krasny (10) developed a treecode-accelerated boundary integral solver for the linear PBE that lowers the computational cost from N^2 to Nlog(N). Pang and Zhou (4) discussed the use of the Van Der Walls surface and the molecular surface for the dielectric boundary. Chen et Al. (15) created a matched interface and boundary based PBE software package that delivers second order convergence. It allows accurate results for a mesh as coarse as 1A. Recently, studies have focused on protein folding for mini-proteins and more complex proteins (12).

1.5 Objective of Study

As discussed above, the linear Poisson Boltzmann equation is used in conjunction with the boundary integral method to solve for the interaction energy between molecules and their ionic environment. The use of the LPB equation limits the solution to low zeta potential problems. With increasing zeta potential, the non-linear Poisson Boltzmann equation increases exponentially faster than the

linearized Poisson Boltzmann equation, rendering the results of the LPBE less accurate in the curtain around the biomolecule.

In order to account for the loss of accuracy when using the LPBE, an interfacial discontinuity condition, described by equations 37, 38 and 39, is introduced. It is then applied to two cases, a sphere in an infinite domain with a central charge and to the interaction of two spherical particles each with a charge.

1.6 Future Work

Multiple avenues still need to be investigated. The present work is limited to idealized geometries. However, many particles involve complex geometries. Additionally, only identical spherical particles were considered. An investigation of the solvation energy for dissimilar particles should be completed.

The methods used in this study can be applied to a wide range of biomolecules, and thus, lead the path to a better understanding of drug delivery systems.

Furthermore, the current analysis is symmetrical with the charge being applied at the center of each sphere. One can examine the energy when the charge is displaced away from the center as happens in electro-fluorescence.

Chapter 2

Governing Equations

2.1 The Non-Linear Poisson Boltzmann Equation

The Poisson Boltzmann equation describes the electrostatic interaction and ionic distribution of a molecule in a solvent at a finite temperature. As an implicit approach, the PBE allows the solute to be modeled as a continuous medium while the solvent is analyzed at an atomic level. The distribution of an electric charge to the resulting electric field is governed by Gauss' law.

$$\nabla \cdot E = \frac{\rho}{\varepsilon} \tag{4}$$

where E represents the electric field, ρ the charge distribution of the molecule and ε the dielectric constant. The dielectric constant accounts for the polarization effect of solvent molecules. Due to the implicit approach pursued, ε is averaged to a constant.

The electric field E is given by

$$E = -\nabla \emptyset \tag{5}$$

Where $\emptyset$ is the electric potential. Substituting 2 into 1yields the Poisson equation:

$$\nabla \cdot \epsilon \nabla \emptyset + \rho = 0 \tag{6}$$

The anions and cations undergo motion due to their electrostatic interaction and the entropic force acting on them. The former encourages the mobile ions to separate orderly, i.e. the anions to migrate to higher potential and

the cations to lower potential, while the latter encourages entropy. This leads to an orderly potential landscape far from the surface of the particle and a double layer near the molecule. This distribution of ions follows the Boltzmann distribution law. Hence, a term ρ_b is added to the equation.

$$\rho_b = \sum_i e v_i c_i \tag{7}$$

where e is the unit charge of a single proton, v the valence, and c the concentration of ions/unit volume. The concentration c is given by the bulk concentration c_o, the Boltzmann constant K and the temperature T. By its definition, ρ_b is absent from the biomolecule and in a layer in the van der walls surface.

$$c_i = c_o e^{\frac{-v e \emptyset}{KT}} \tag{8}$$

For a 1:1 electrolyte solution, $v_1 = -v_2 = 1$ and ρ_b becomes

$$\rho_b = e v_1 c_1 + e v_2 c_2 \tag{9}$$

$$= c_o e \left(e^{\frac{-e \emptyset}{KT}} - e^{\frac{e \emptyset}{KT}} \right) \tag{10}$$

2.2 Normalizing the Poisson Boltzmann Equation.

Let a be a characteristic length used to normalize the radius of the sphere, such that:

$$r = a \bar{r} \tag{14}$$

And k to be calculated such that:

$$k^2 = \frac{2c_o e^2}{\varepsilon KT} \tag{15}$$

Furthermore, let there be a $\bar{k}$ such that:

$$\bar{k} = ak \tag{16}$$

Note that $\frac{1}{k}$ measures the electrostatic effect of a charge and the length at which it persists, also known as the Debye length. Equation 11 is the non-linear Poisson Boltzmann equation (NLPB). It neglects the effects of non-Columbic interactions and the correlation between an ion and its own ionic atmosphere. These effects are best represented by quantum mechanics.

Let the potential and the density be normalized respectively by

$$\bar{\emptyset} = \frac{e\emptyset}{KT} \tag{17}$$

And

$$\bar{\rho} = \frac{e\rho}{\varepsilon KT} \tag{18}$$

The Boltzmann density becomes

$$\rho_b = c_o e\left(e^{-\bar{\emptyset}} - e^{\bar{\emptyset}}\right) \tag{19}$$

$$= -2c_o e \sinh\bar{\emptyset} \tag{20}$$

Equation 10 becomes

$$\nabla^2\bar{\emptyset} + \frac{\rho}{\varepsilon} - \frac{2c_o e}{\varepsilon}\sinh\bar{\emptyset} = 0 \tag{21}$$

$$\nabla^2\bar{\emptyset} + \bar{\rho} - k^2\sinh\bar{\emptyset} = 0 \tag{22}$$

The displacement and electric field are also normalized using:

$$E = \frac{K_B T}{ea} \bar{E} \tag{23}$$

And

$$D = \frac{\epsilon K_B T}{ea} \bar{D} \tag{24}$$

For a 1:1 electrolyte solvent, the solution to the PBE for a one dimensional

problem with boundary conditions as listed in equation 26 is given by:

$$\bar{\emptyset} = 4 \tanh^{-1} \left[\tanh\left(\frac{\bar{\emptyset}_o}{4}\right) e^{-\bar{k}\bar{z}} \right] \tag{25}$$

And the displacement D is given by:

$$\bar{D} = \frac{4\bar{k} \tanh\left(\frac{\bar{\emptyset}_o}{4}\right) e^{-\bar{k}\bar{z}}}{1 - \tanh^2\left(\frac{\bar{\emptyset}_o}{4}\right) e^{-2\bar{k}\bar{z}}} \tag{26}$$

Where $\bar{\emptyset}_o$ is the normalized electric potential on the surface and $\bar{z}$ is the

normalized distance S.T:

$$z = a\bar{z} \tag{27}$$

2.2 The Linear Poisson Boltzmann Equation

In the case of weak electrostatic potential, $\sinh \bar{\emptyset} \approx \bar{\emptyset}$ and the NLPB is

linearized to

$$\nabla^2 \bar{\emptyset}_l + \bar{\rho} - k^2 \bar{\emptyset}_l = 0 \tag{25}$$

where the subscript l represents the linearized approximation.

The linearized Poisson Boltzmann equation (LPBE) above can easily be

solved analytically for a sphere with a central point charge. Let the potential at the

surface be a value $\overline{\emptyset}_{l0}$, and the potential in the far field be 0, the boundary conditions are:

$$\begin{cases} At\ z = 0, \overline{\emptyset} = \overline{\emptyset_{lo}} \\ At\ z = \infty, \overline{\emptyset} = 0 \end{cases} \tag{26}$$

The Solution to the LPBE is then given by

$$\overline{\emptyset}_l = \overline{\emptyset}_{l0} e^{-kz} \tag{27}$$

The electric displacement D is related to the electric field E by

$$D = \epsilon E \tag{28}$$

Thus,

$$\overline{D}_l = \epsilon k \overline{\emptyset}_{l0} e^{-kz} \tag{29}$$

2.4 The potential Energy Density

　　　The potential energy W of the system described by the Poisson Boltzmann equation is obtained from adding the electrostatic energy due to the linear polarization, the effect of charge induction in an electrolyte and the work of free charges. It can be written as follows:

$$w = -\int_0^E D \cdot dE + \int_0^{\emptyset} \rho_b d\emptyset + \rho_f \emptyset \tag{30}$$

Substituting equations 20 and 28, normalizing and integrating yields a solution for the non-linear Poisson Boltzmann of:

$$\overline{w} = -\frac{1}{2}\overline{D} \cdot \overline{E} - \overline{k}^2 \big[cosh(\overline{\emptyset}) - 1\big] + \overline{\rho}_f \overline{\emptyset} \tag{31}$$

15

Likewise, integrating equation 23 for the linear Poisson Boltzmann Equation yields a linear energy density W of:

$$\bar{w}_l = -\frac{1}{2}\bar{D}_l \cdot \bar{E}_l - \frac{1}{2}\bar{k}^2\bar{\emptyset}_l^2 + \bar{\rho}_f\bar{\emptyset}_l \tag{32}$$

Where

$$w = \frac{\varepsilon k_B^2 T^2}{e^2 a^2}\bar{w} \tag{33}$$

The electrostatic potential energy density per unit surface area, $\bar{\gamma}$, is obtained from integrating $\bar{w}$ along $\bar{z}$ and setting $\bar{\rho}_f$ equal to zero as shown in the following equations

$$\bar{\gamma} = \int_0^\infty \bar{w} d\bar{z} \tag{34}$$

$$= \frac{-8\bar{k}\tanh^2\left(\frac{\bar{\emptyset}_o}{4}\right)}{1-\tanh^2\left(\frac{\bar{\emptyset}_o}{4}\right)} \tag{35}$$

Similarly, the linear electrostatic potential energy density per unit area, $\bar{\gamma}_l$ is

$$\bar{\gamma}_l = -\frac{1}{2}\bar{k}\bar{\emptyset}_{lo}^2 \tag{36}$$

The boundary condition used at $z = \infty$, states that the potential is negligible far away from the sphere for both the LPBE and NLPBE. Setting the potential equal at large $\bar{z}$ yields a relationship between $\bar{\emptyset}_{lo}$ and $\bar{\emptyset}_o$, $\bar{D}_{lo}$ and $\bar{D}_o$ and $\bar{\gamma}_{lo}$ and $\bar{\gamma}_o$ S.T:

$$\bar{\emptyset}_{lo} = 4\tanh\frac{\bar{\emptyset}_o}{4} \tag{37}$$

$$\bar{D}_{lo} = \left[1 - \tanh^2\left(\frac{\bar{\emptyset}_o}{4}\right)\right]\bar{D}_o \tag{38}$$

$$\bar{\gamma}_{lo} = \bar{\gamma}_o + \frac{8\bar{k}\tanh^4\left(\frac{\bar{\phi}_o}{4}\right)}{1-\tanh^2\left(\frac{\bar{\phi}_o}{4}\right)} \tag{39}$$

Chapter 3

Results

3.1 Validation of the code used to obtain the results: Kirkwood Case

The solvation energy of a single sphere with a central charge has been
solved analytically by Kirkwood (6). In this first part of the results, we validate
the code and methods used by comparing the analytical solvation energy to the
one obtained numerically. A table of the properties used is shown below.

Table 1: Properties of Case 1

Property	Description	Value
Q	Charge	50e
e	Electric charge	1.602e-19 (V/m)^2
ε_1	Dieletric constant of the particle	80 F/m
ε_2	Dielectric constant of the electrolyte	2 F/m
K_B	Boltzmann Constant	1.381e-23 (J/atom*K)
T	Temperature	300K
$\bar{k}$	1/Debye length	6.285 (1/$\dot{A}$)

The table below shows the results obtained using a 24*24 mesh size. This
particular mesh size is used due to its low error and its lower computational cost.
The error is calculated using the formula below:

$$e_{sol} = \frac{e_{analytical} - e_{numerical}}{e_{analytical}} \qquad (33)$$

Table 2: Validation of Method Used

Analytical Solution	48130 J/mol
Numerical Solution	48901 J/mol
Error	1.6%

Let's consider the effect of the mesh size on the accuracy of the results

obtained. Four different mesh sizes were used and the results of the solvation

energy were plotted as shown below.
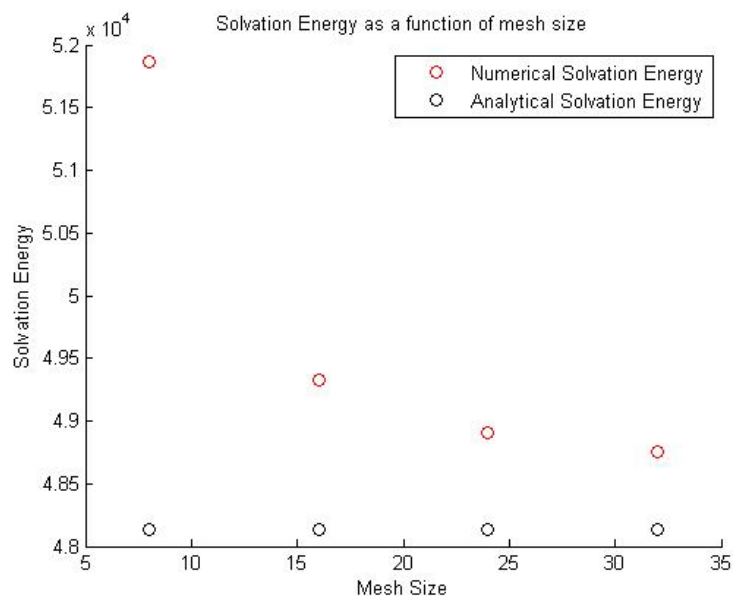
Figure 8: Solvation Energy vs. the mesh size

As is expected, the numerical solution is improved with the use of a higher

mesh size. In order to choose the best one in terms of computational cost, the

solvation energy error for each mesh was calculated and plotted. As is evident
from the plot below, the 24*24 mesh size was within a 2% error. This led to its
use for the remainder of the results.
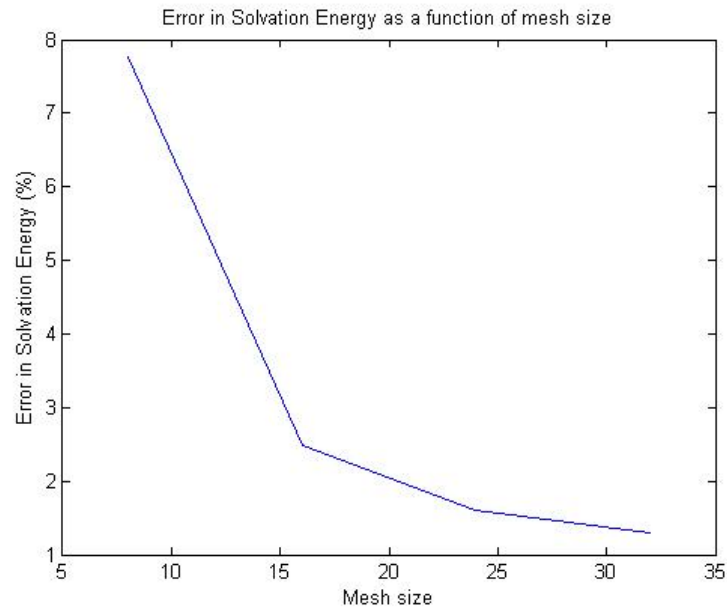
Figure 9: Error in Solvation Energy as a function of mesh size

A surface plot and a contour plot of the potential were created and can be
seen below. The maximum potential is found at the center of the sphere, where
the charge is located and has a value of 5011.6 V.
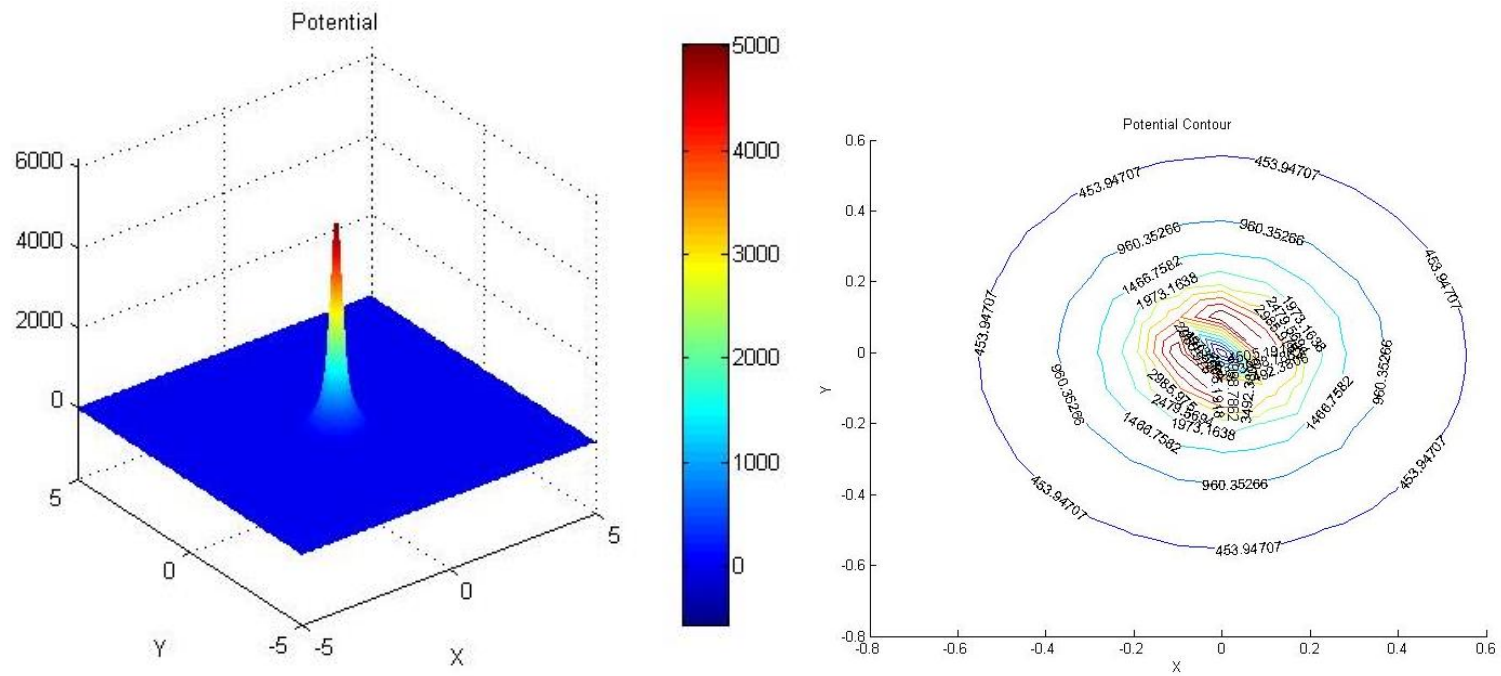
Figure 10: Surface (left) and Contour (right) plots of the Potential Field for the Kirkwood Case.

3.2 One spherical particle with a central charge

3.2.1 The effect of $\bar{k}$ and ε on the solvation energy

As mentioned earlier, $\frac{1}{\bar{k}}$ is an important parameter known as the Debye length. It measures the effect of the ratio of the competing electrostatic interaction force and the thermal force. In the following section, the influence of $\bar{k}$ and the dielectric constant on the solvation energy will be discussed. Since the solvation energy is the sum of the energy of fixed charges, represented by the dielectric constant, and the energy of the mobile ions, represented by $\bar{k}$, the first results will have $\bar{k}$ kept constant as the charge magnitude increases. In the second section, the dielectric constant will be kept constant and $\bar{k}$ and the charge magnitude will vary. Both the linear and the non-linear PBE will be plotted.

Let us consider sixteen cases with the following parameters. Table 3 shows the $\bar{k}$ and ε parameters used. For each dielectric ratio, four Debye lengths are applied and the results plotted.

Table 3: $\bar{k}$ and ε Parameters

Case #	$\bar{k}$ $(1/\dot{A})$	ε	Object
1	0.1,1,10,1000	0.025	Biomolecule
2	0.1,1,10,1000	0.32	Potassium nitrate
3	0.1,1,10,1000	1	Electrolyte
4	0.1,1,10,1000	3	A material three times more polar than water

3.2.1.1 Constant Debye length and varying dielectric constant and charge magnitude
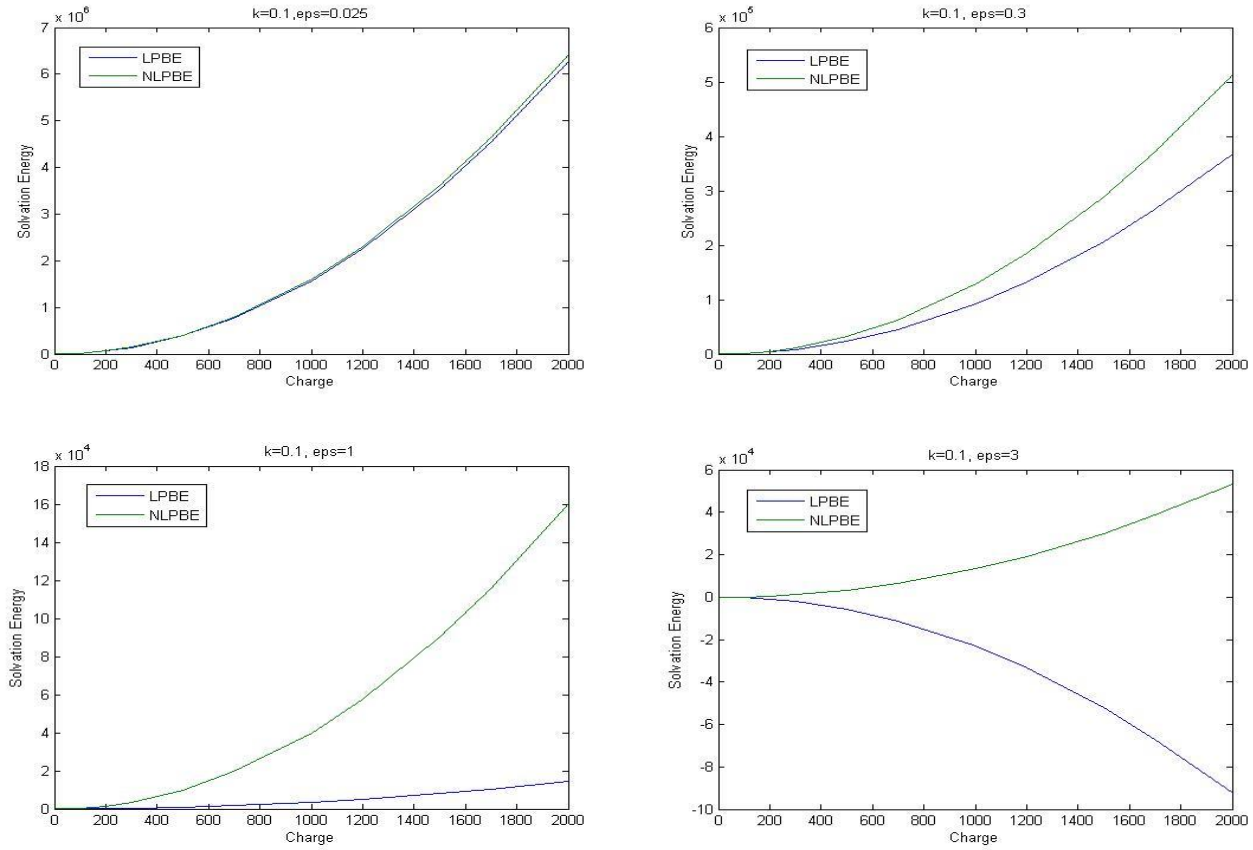
Figure 11: The Solvation Energy for the LPBE and NLPBE for Case 1
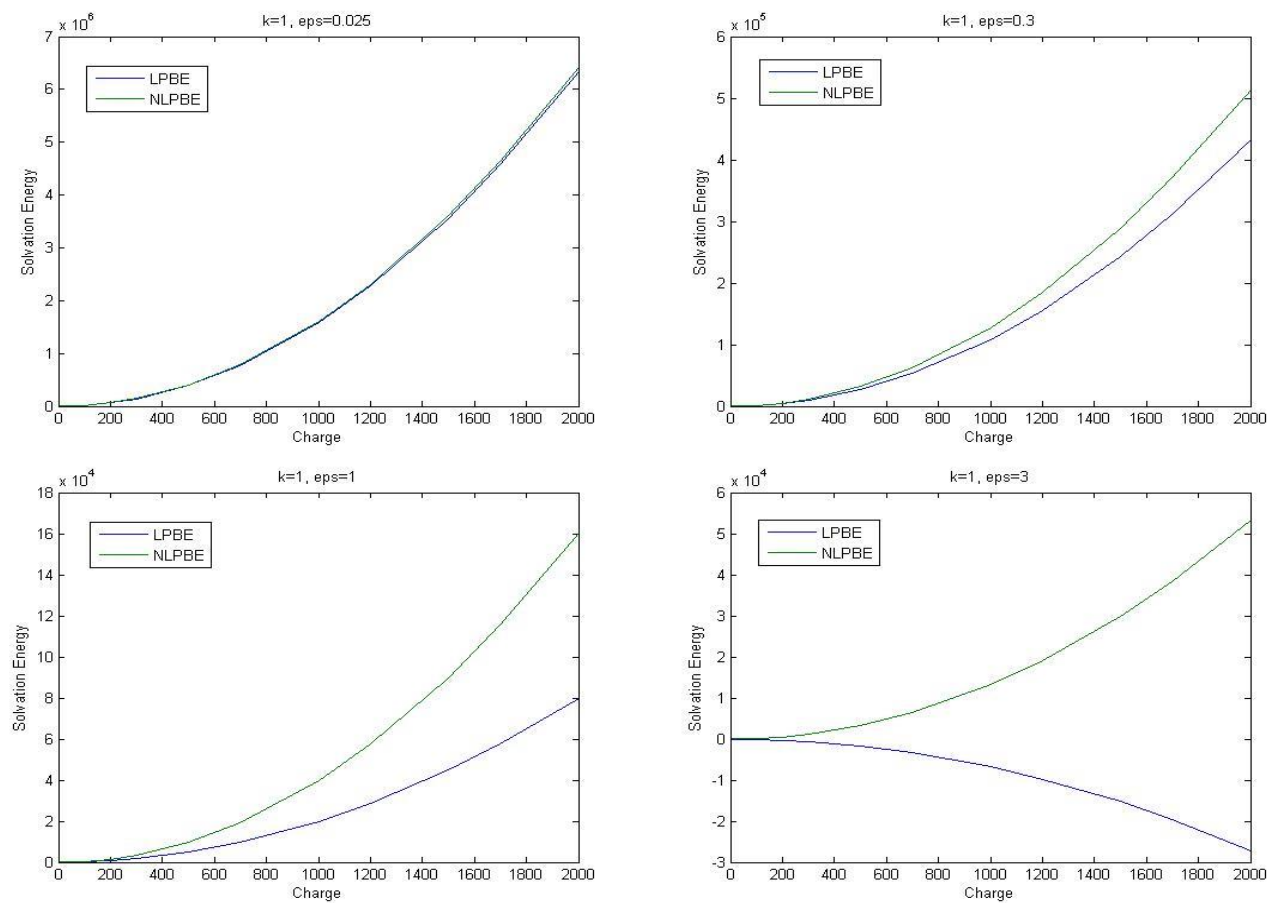
Figure 12: The Solvation Energy for the LPBE and NLPBE for Case 2
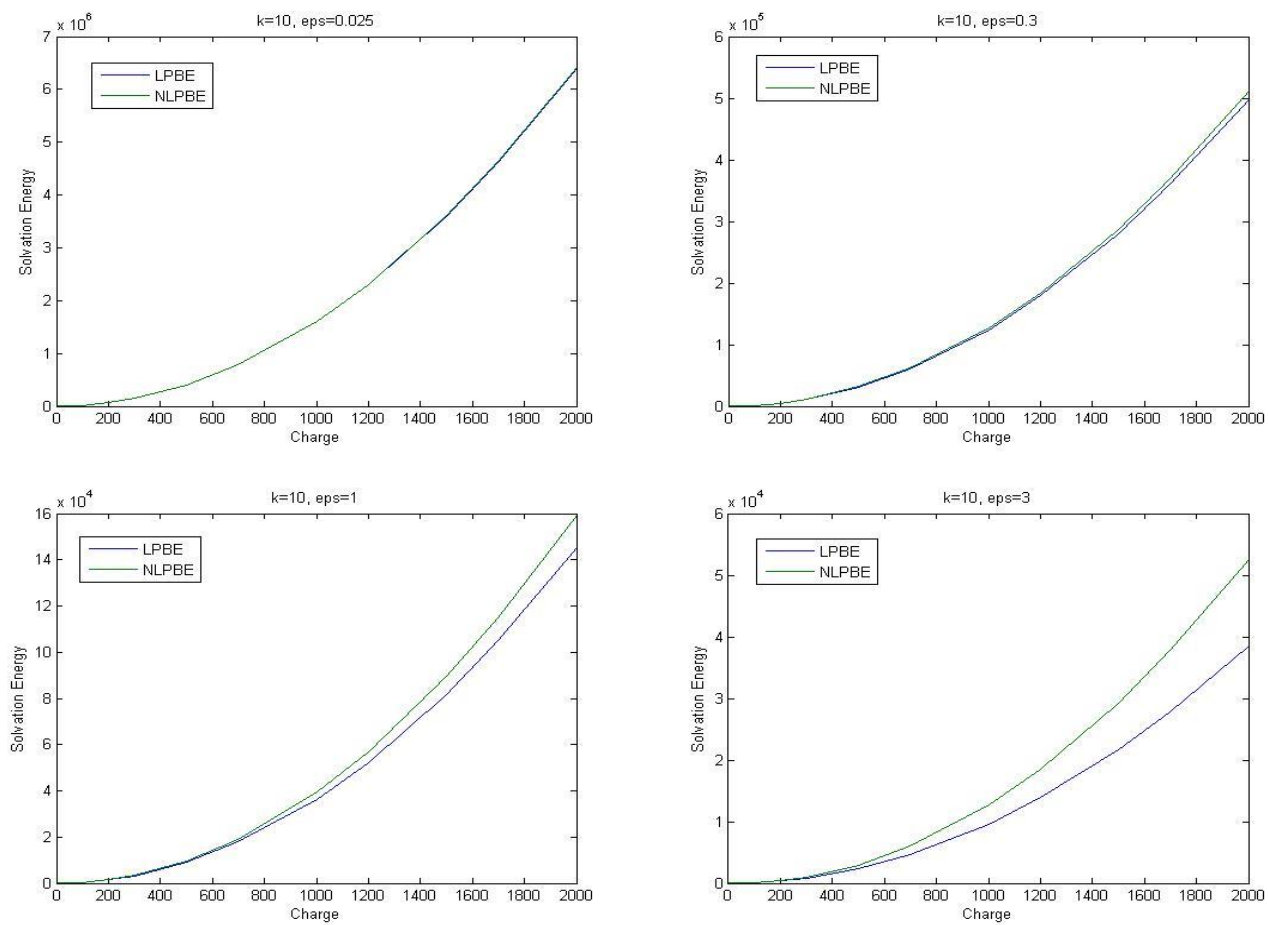
Figure 13: The Solvation Energy for the LPBE and NLPBE for Case 3
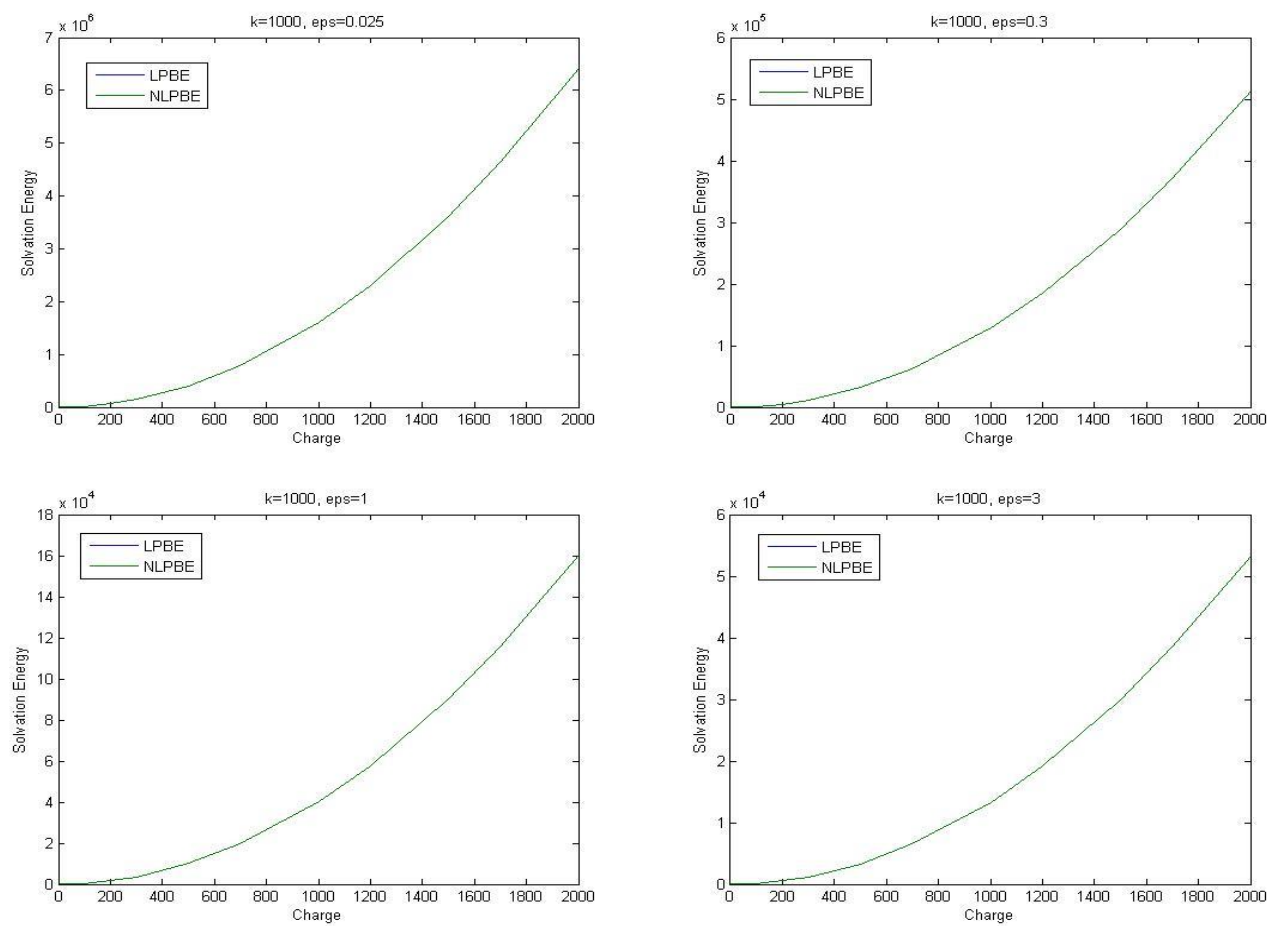
Figure 14: The Solvation Energy for the LPBE and NLPBE for Case 4

As can be seen from the above plots, in general, as $\bar{k}$ stays constant and ε increases, there is a divergence between the solution for the linear Poisson Boltzmann Equation denoted by the blue lines and the nonlinear PBE denoted by the green lines. Specifically, the solvation energy of the NLPBE increases. Please note that the convention used for the solvation energy allows for higher solubility as the solvation energy increases.

When the Debye length is very small and thus $\bar{k}$ is very large, the increase of the dielectric constant from 0.025 to 3 does not impact the results. In this case, the effect of the dielectric constant on the solvation energy is very small relative to the effect of the Debye length. This is in contrast to when the Debye length is very large and an increase in the dielectric constant significantly alters the results of the nonlinear PBE.

It can be noticed that there is an irregularity when the Debye length is large or $\bar{k}$ is small and the dielectric constant is large. It will be discussed in the section below.

3.2.1.2 Constant Dielectric Constant and varying Debye length and charge magnitude

In this section, the plots of the solvation energy are grouped by constant dielectric constant and varying Debye lengths. The irregularity in the case of high dielectric constant and low $\bar{k}$ is discussed.

27
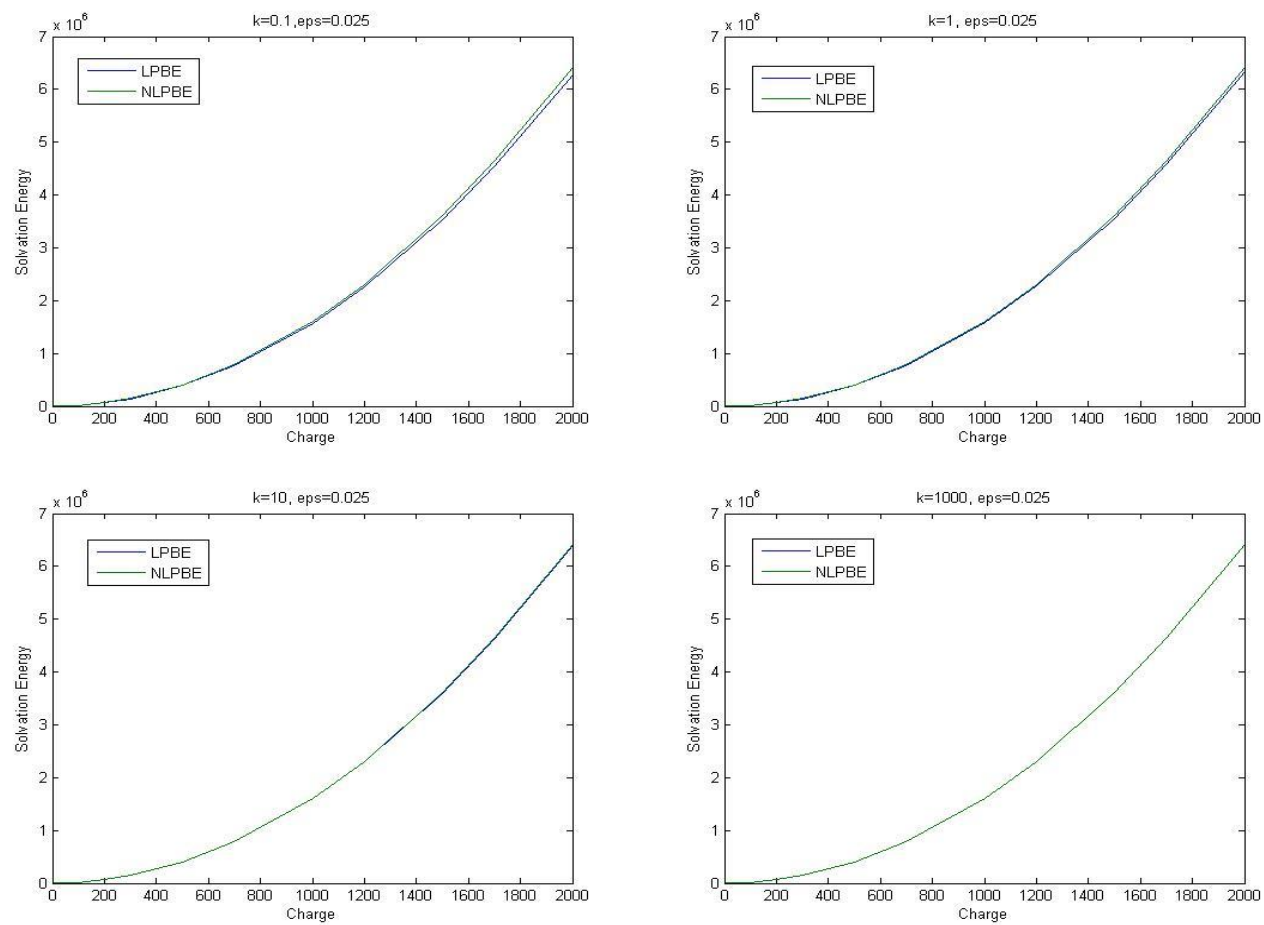
Figure 15: Solvation Energy Calculated by the LPBE and NLPBE for ε=0.025
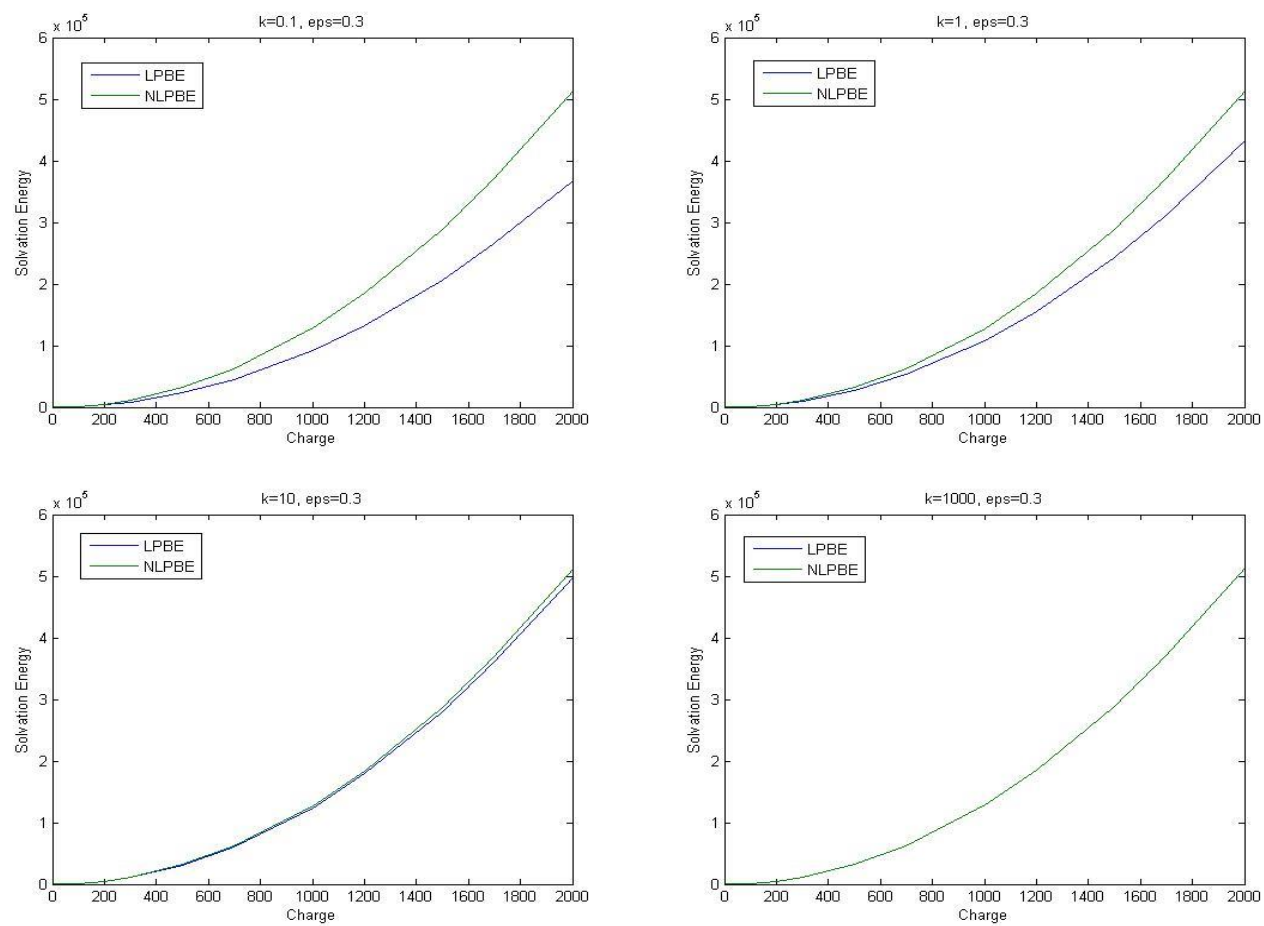
Figure 16: Solvation Energy Calculated by the LPBE and NLPBE for ε=0.31
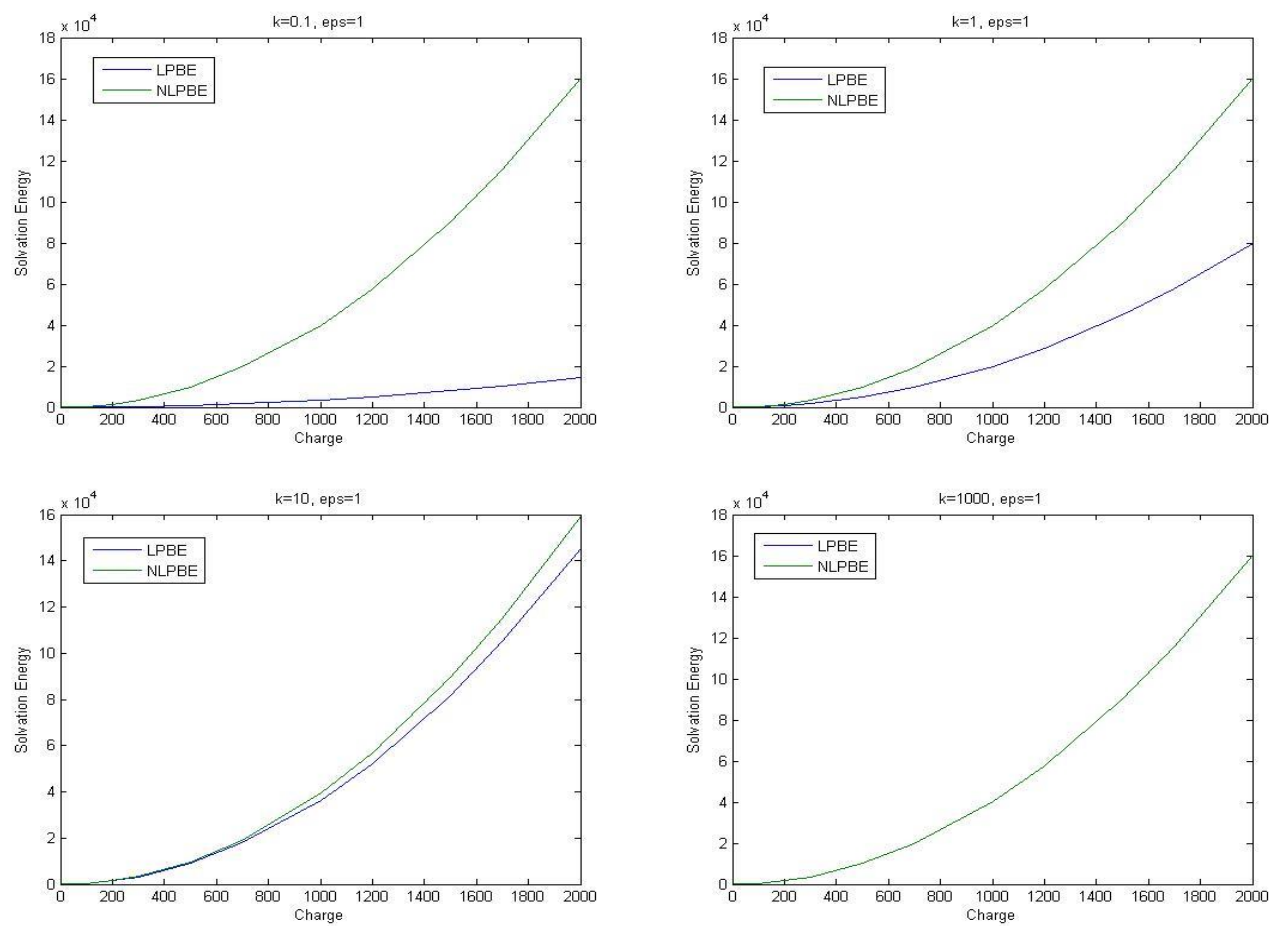
Figure 17: Solvation Energy Calculated by the LPBE and NLPBE for ε=1
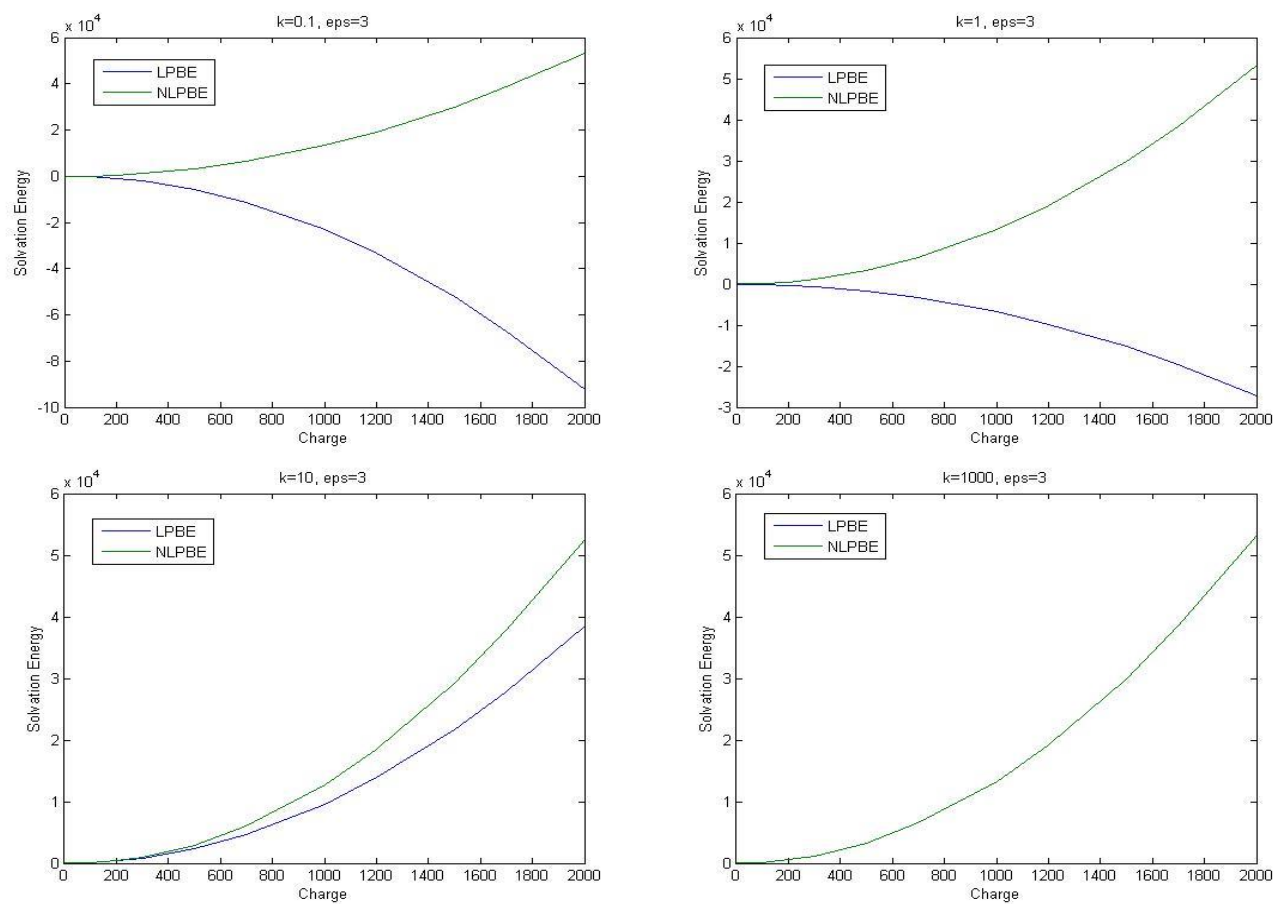
Figure 18: Solvation Energy Calculated by the LPBE and NLPBE for ε=3

As can be seen from the plots above, when ε stays constant, an increase in $\bar{k}$ decreases the gap between the solution for the solvation energy for the LPBE and the approximation for the NLPBE. As $\bar{k}$ increases, the portion of the solvation energy that is dependent on the Debye length becomes smaller and the portion of the solvation energy that is dependent on the dielectric constant becomes more pronounced.

Let's take a closer look at the solution for high Debye length and a high dielectric constant. A magnified look at the solvation energy for charges below 100 C, a high dielectric constant of 3, and a $\bar{k}$ of one can be seen below. A logarithmic scale of the results is also plotted. Please note that for easier viewing, the convention sign for the solvation energy was reversed in the enlarged and the logarithmic plots.
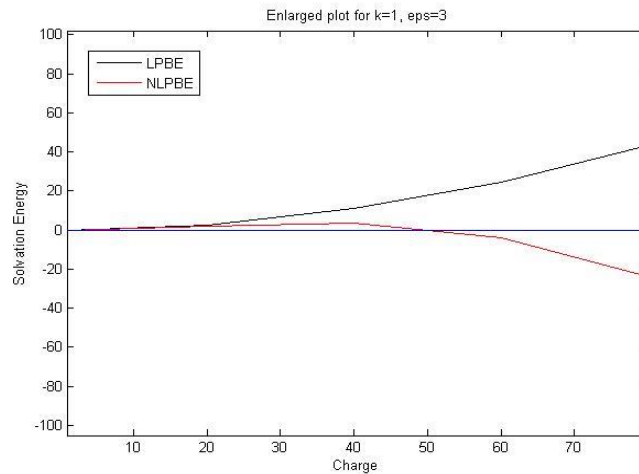
Figure 19: A Magnified View of the Solvation Energy for Low Debye Length and High Dielectric Ratio
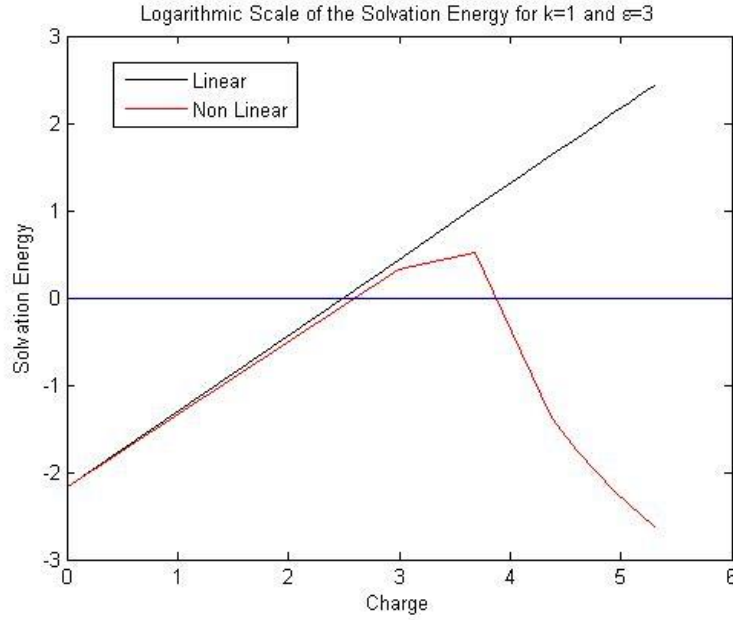
Figure 20: Logarithmic Scale of the Solvation Energy for Low Debye Length and

High Dielectric Ratio

As can be seen from the two plots above, the NLPB solution initially

increases as the charge increases, similarly to the LPBE, then decreases with a

further increase in the charge magnitude. When the dielectric ratio is higher than

one, the particle is more polar than the electrolyte solution. This condition

coupled with a low charge means that the particle does not dissolve

instantaneously in the solution. As the particle becomes highly charged, it is more

adept at attracting or repelling ions. This leads to sharp decrease in the solvation

energy of the nonlinear PBE and faster dissolution of the particle.

3.2.1.3 A look at the potential field.

A few cases were chosen to demonstrate the effect of the Debye length and the dielectric ratio on the potential field. Each case contains a varying parameter while the other two remain constant. For example, for case 1, the nonlinear PBE was solved for a dielectric ratio of 0.3, a $\bar{k}$ of 1000 $\frac{1}{\dot{A}}$ and a charge of 1500 C. Then for the same $\bar{k}$ and Q, the dielectric ratio was changed to 1 and the results of the surface potential and the potential contour were compared. Note that only the nonlinear PBE was considered. The table below shows the parameters used for each case.

Table 4: Parameters Used for the Solution to the Potential Field

Case number	ε	$\bar{k}$ (1/$\dot{A}$)	Q (C)
1	0.3	1000	1500
	1	1000	1500
2	0.025	10	200
	0.025	10	2000
3	0.31	0.1	500
	0.31	10	500
4	3	1	40
	3	1	200

Case 1:
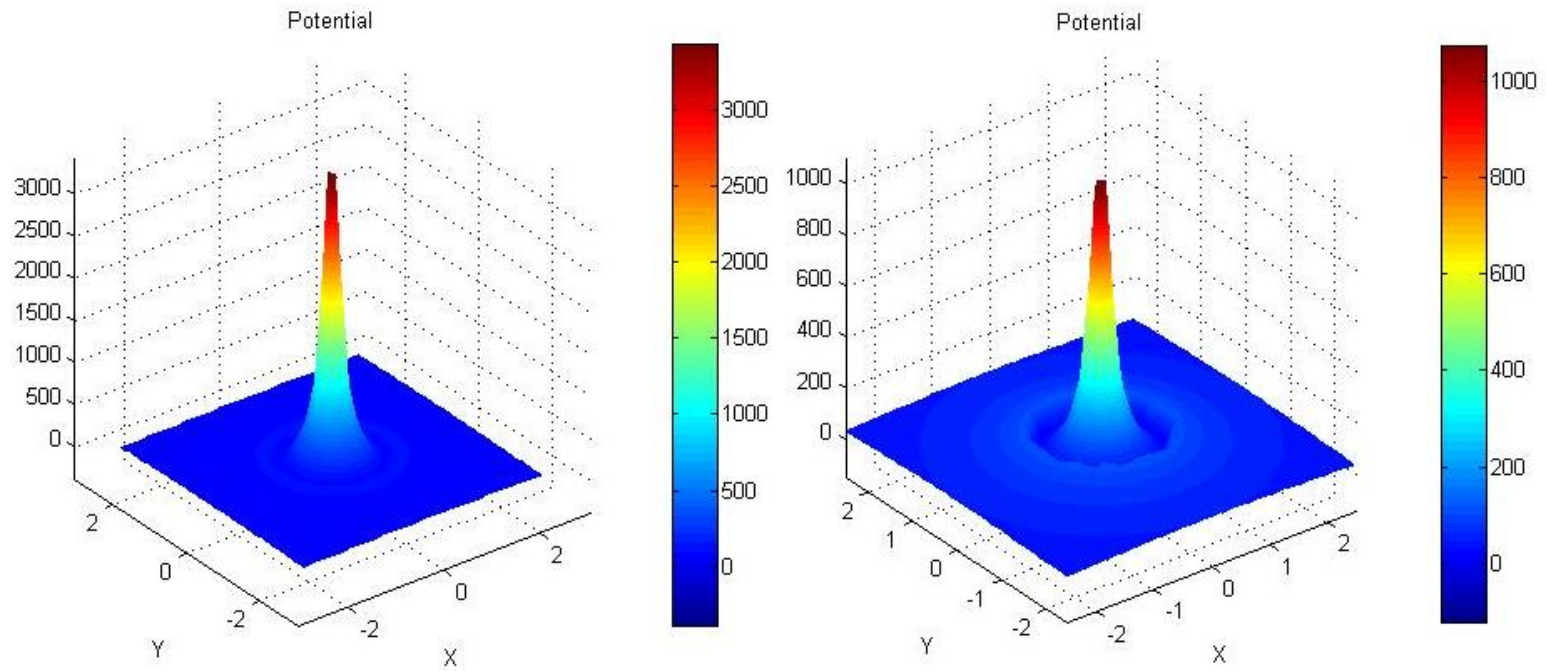
Figure 21: Potential Field for Case 1. On the Left, ε=0.31, and The Image on the Right Contains ε=1
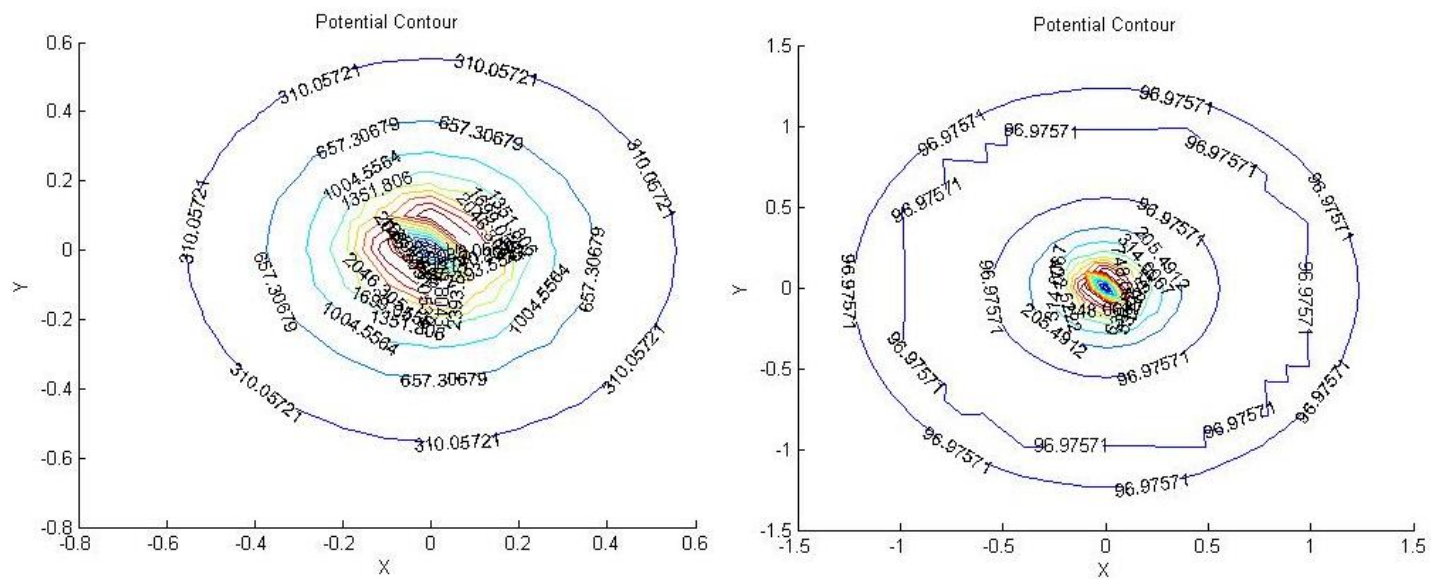
Figure 22: Contour Plot of the Potential Field for Case 1. The Left Image has a Dielectric Ratio of 0.31, While for the

Right Image ε=1

In the case of high dielectric mismatch and the dielectric ratio is less than one, the potential reaches a maximum of approximately 3000 V at the center of the sphere where the charge is located. It decreases as the distance from the center increases. It reaches a minimum of 310 V a distance 0.6 from the charge. For the same Debye length, removing the dielectric mismatch lowers the maximum potential by two thirds. However, the potential is induced a farther distance. One can also see a crater like distribution at the boundary of the particle.

Case 2
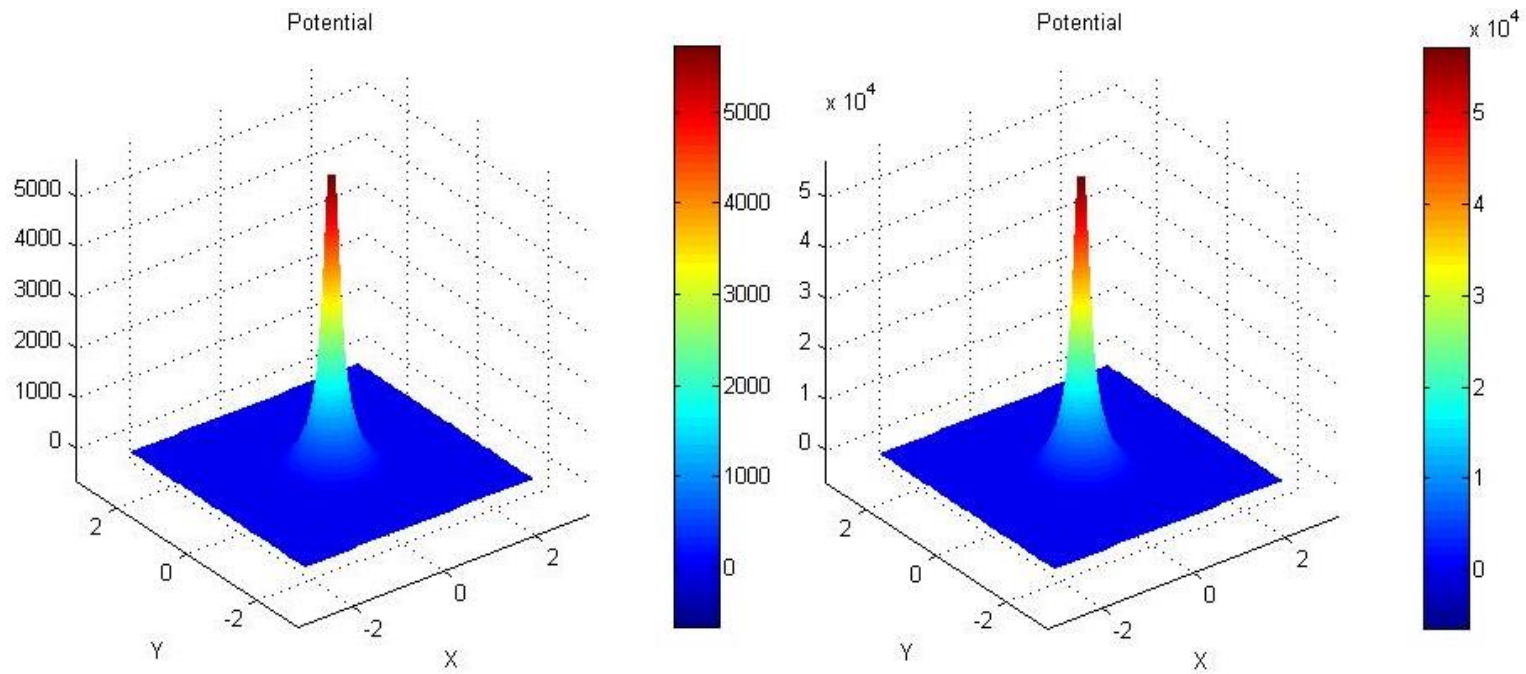
Figure 23: Surface Plot of the Potential Field for Case 2. A Relatively Small Charge (200 C) Was Applied to the Left

Image, While the Right Image Experienced a High Charge of 2000 C.
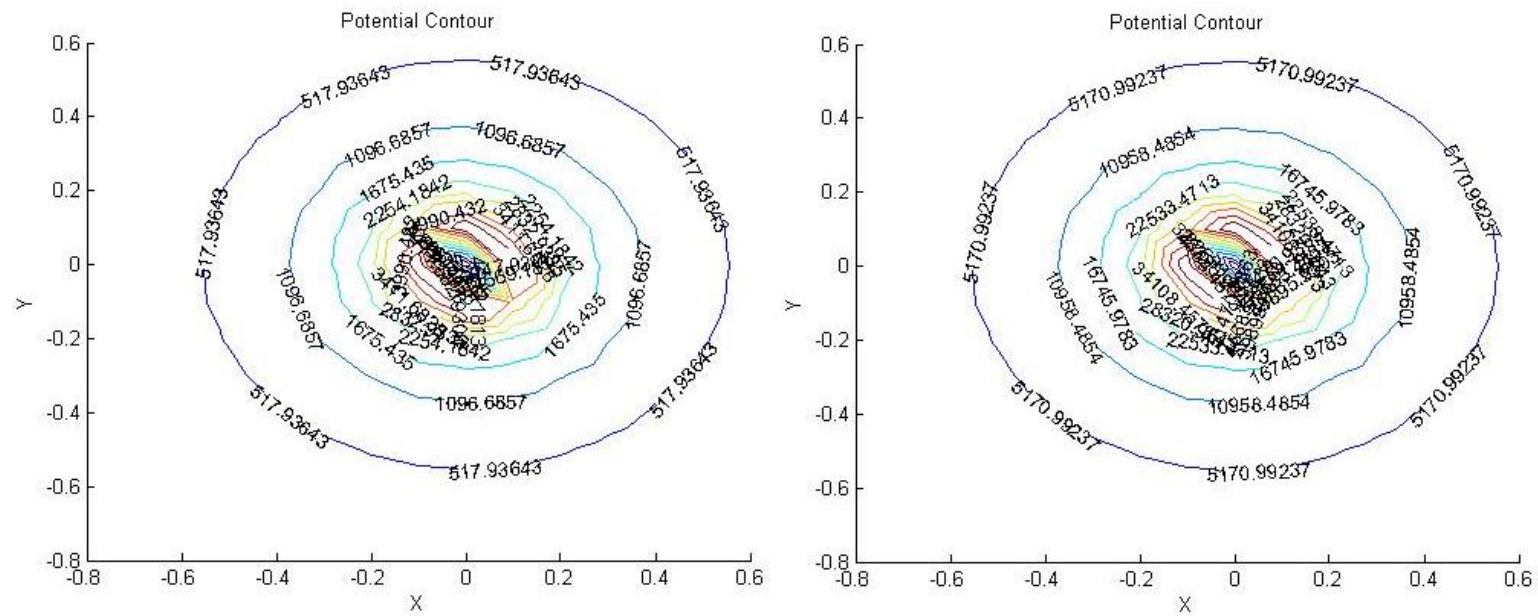
Figure 24: Contour Plot of the Potential Field. The Left Image Corresponds To a Charge of 200 C While the Right

Image Experienced a Charge Of 2000 C

Case 2 is rather straight forward. It can be seen that the potential is proportional to the charge applied. An increase in the charge by a factor of 10 leads to an increase in the potential by a factor of 10. In both plots above, it can be seen that the potential is maximum at the center of the particle where the charge is applied and decreases as the distance from the center increases.

Case 3
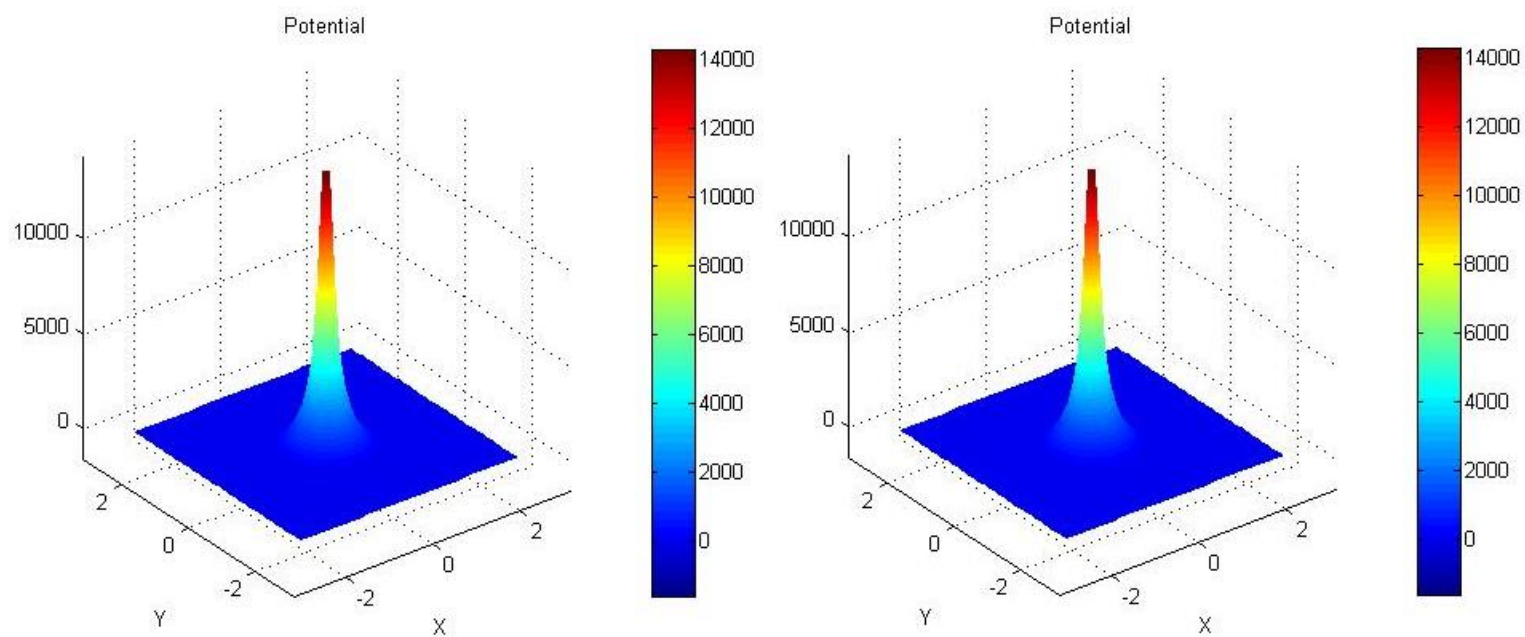
Figure 25: Surface Plot of the Potential Field for Case 3. The Right Image Has a Debye Length of 10 $\mathring{A}$, Whereas the

Left One Has a Debye Length of $0.1\mathring{A}$

Figure 26: Contour Plot of the Potential Field for Case 3. The Left Image Has a Debye Length of 10 $\mathring{A}$, While the Right

Image Has a Debye Length Of 0.1$\mathring{A}$

It is evident from both the surface and the contour plot of the potential field that an increase of $\bar{k}$ in the case of high dielectric mismatch has little effect on the value of the potential. In both $\bar{k}=0.1$ and $\bar{k}=10$, the maximum potential is located at the center of the sphere with a magnitude of approximately 14000 V. It decays outwards from the center to a min of 1298 V in the case of $\bar{k}=0.1$ and 1294 V in the case of $\bar{k}=10$, a decrease of approximately 0.3%.

Case 4
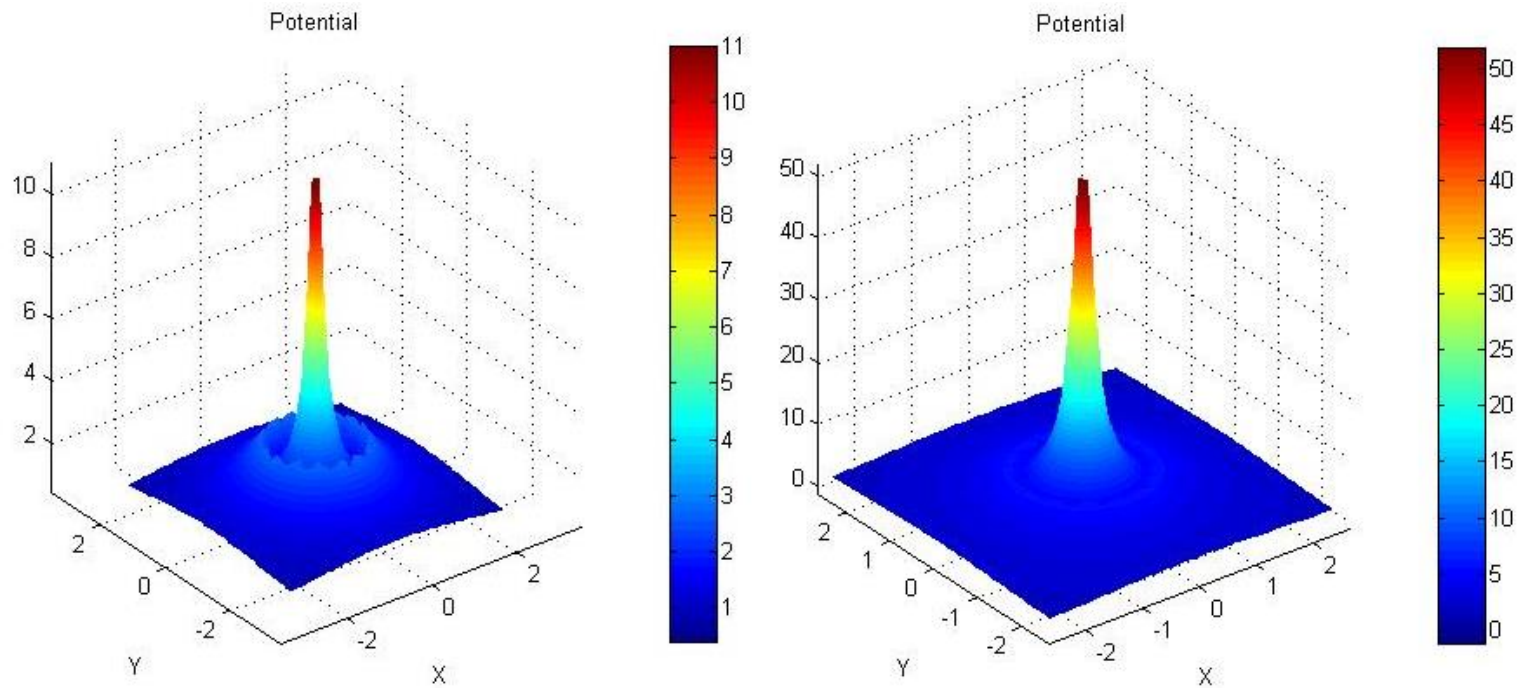
Figure 27: Surface Plot of the Potential Field for Case 4. The Left Image Represents a Charge of 40 C Whereas the

Right Image Contains a Charge of 200 C.
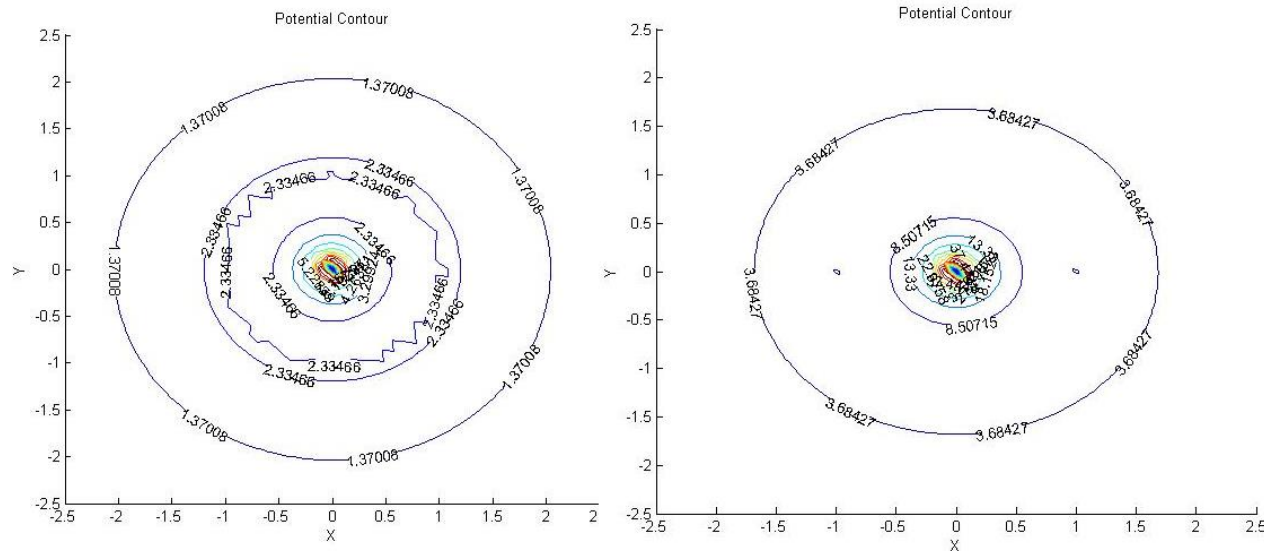
Figure 28: Contour Plot of the Potential Field for a High Debye Length and a High Dielectric Ratio. The Image on the

Left was Assigned a Charge of 40 C While the Right Image Experienced a Charge of 200 C

When the dielectric ratio is three and the charge is low, there is a crater effect near the boundary of the particle.

The contour is no longer circular at the boundary. The potential increases as it approaches the center of the sphere

where it reaches a maximum of approximately 11V. When the charge is increased to 200C, the potential increases to

about 50V. The contour image shows two circular potentials near the boundary although that could be simply a

fragment.

3.3 Two Spherical Particles

Let there be two identical, spherical, charged particles a distance a from each other, as shown in figure 29. Both particles have similar dielectric constants and are present in an electrolyte solution. The parameters used are shown in the table below.

Table 5: Parameters Used for the Two Spherical Particles

ε=0.025		ε=1	
$\bar{k}$ (1/$\dot{A}$)	a ($\dot{A}$)	$\bar{k}$ (1/$\dot{A}$)	a ($\dot{A}$)
0.1	0.1	0.1	0.1
	0.5		0.5
	1		1
	2		2
1	0.1	1	0.1
	0.5		0.5
	1		1
	2		2
10	0.1	10	0.1
	0.5		0.5
	1		1
	2		2
1000	0.1	1000	0.1
	0.5		0.5
	1		1
	2		2
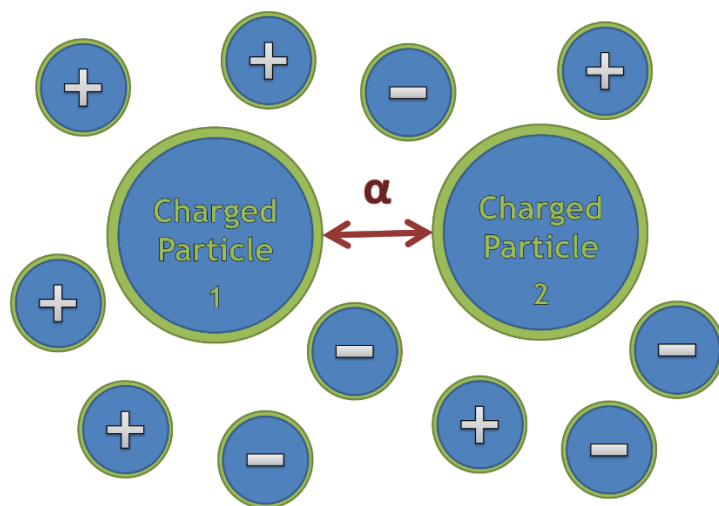
Figure 29: Schematics of the Two Particle Model

Using the above parameters, a comparison of the solvation energy for the linear and nonlinear PBE is made. The interaction energy between the particles is then extrapolated. For each dielectric ratio, the Debye length and the distance between the two particles vary.

3.3.1 Solvation Energy
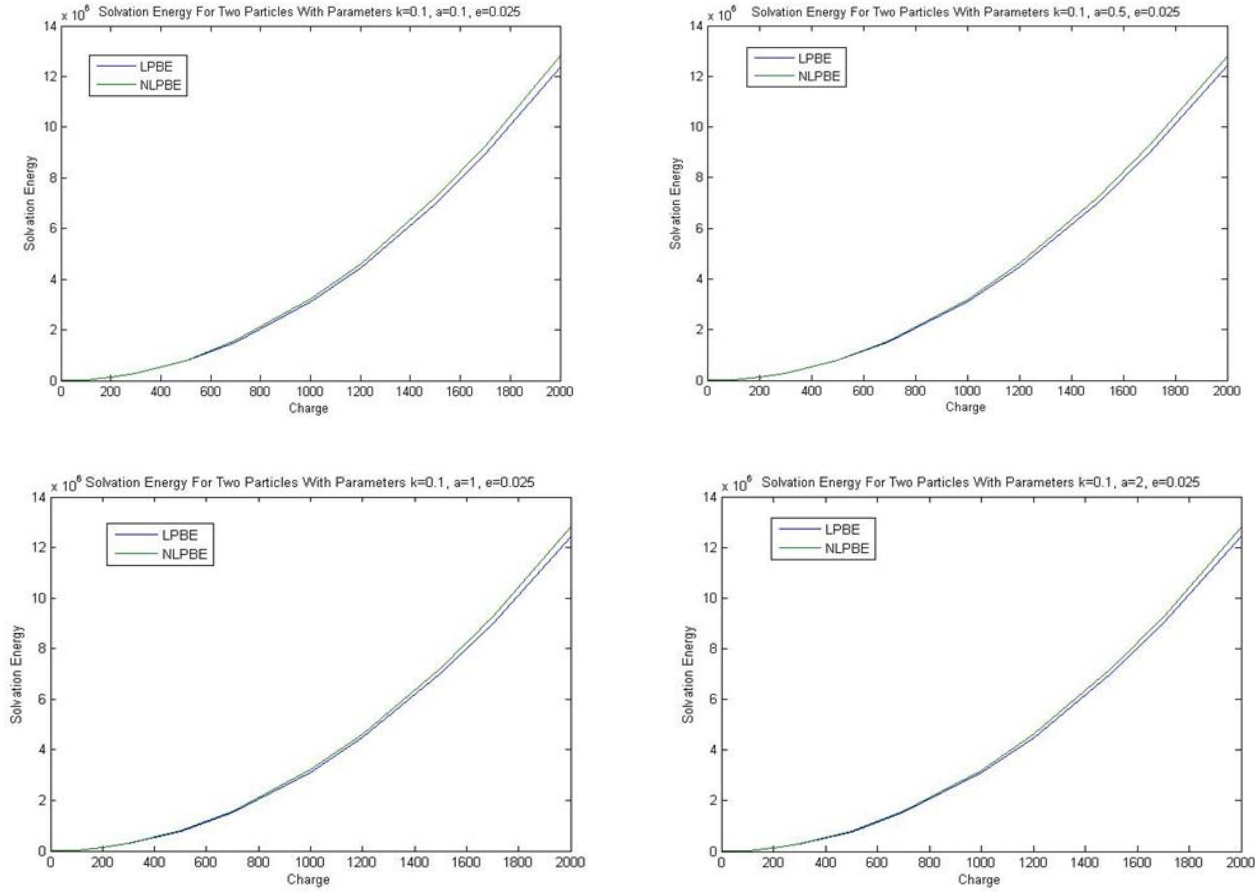
Figure 30: Solvation Energy for Two Particles with Parameters $\bar{k}$=0.1 and ε=0.025. a Varies Clockwise: 0.1, 0.5, 1 to 2
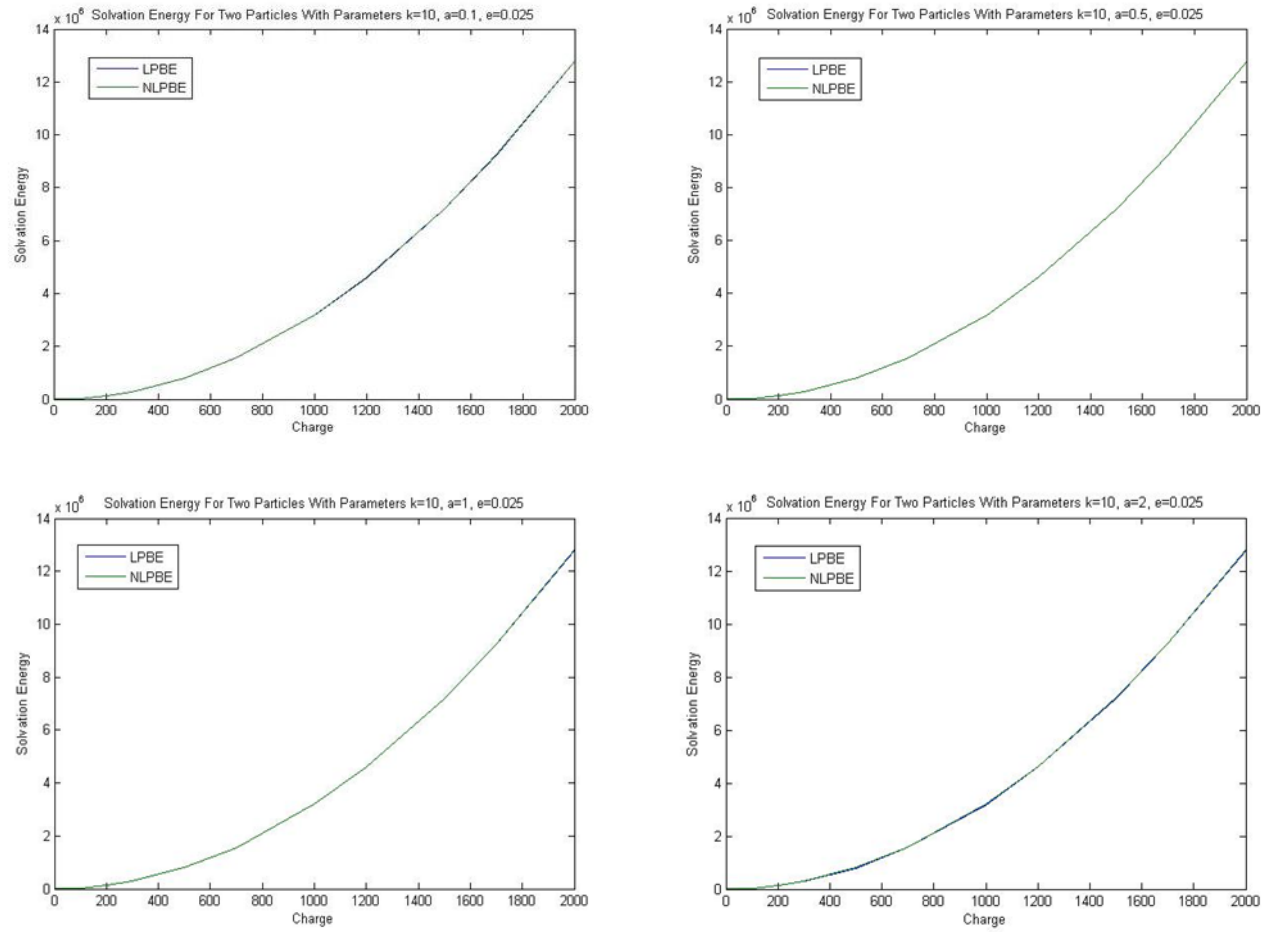
Figure 31: Solvation Energy for Two Particles with Parameters $\bar{k}$=10 and ε=0.025. a Varies Clockwise: 0.1, 0.5, 1 to 2

As can be seen from the eight figures above, the location of the spheres makes little difference in the solvation energy when the dielectric ratio is very small and the Debye length is large. This is because the dielectric ratio is the principal driver of the solvation energy in this case. While in each case, the solvation energy looks the same, it is important to note that there is a difference albeit very small. The difference is much more noticeable when there is no dielectric mismatch as will be discussed later.

Let's look at what happens when $\bar{k}$ increases but the distance between particles and the dielectric ratio stay constant. As can be seen from the following slides, an increase in $\bar{k}$ decreases the gap between the solution to the linear and nonlinear PBE. This is due to the relative contribution of $\bar{k}$. As discussed in the one particle case, an increase in $\bar{k}$ increases its contribution to the solvation energy.
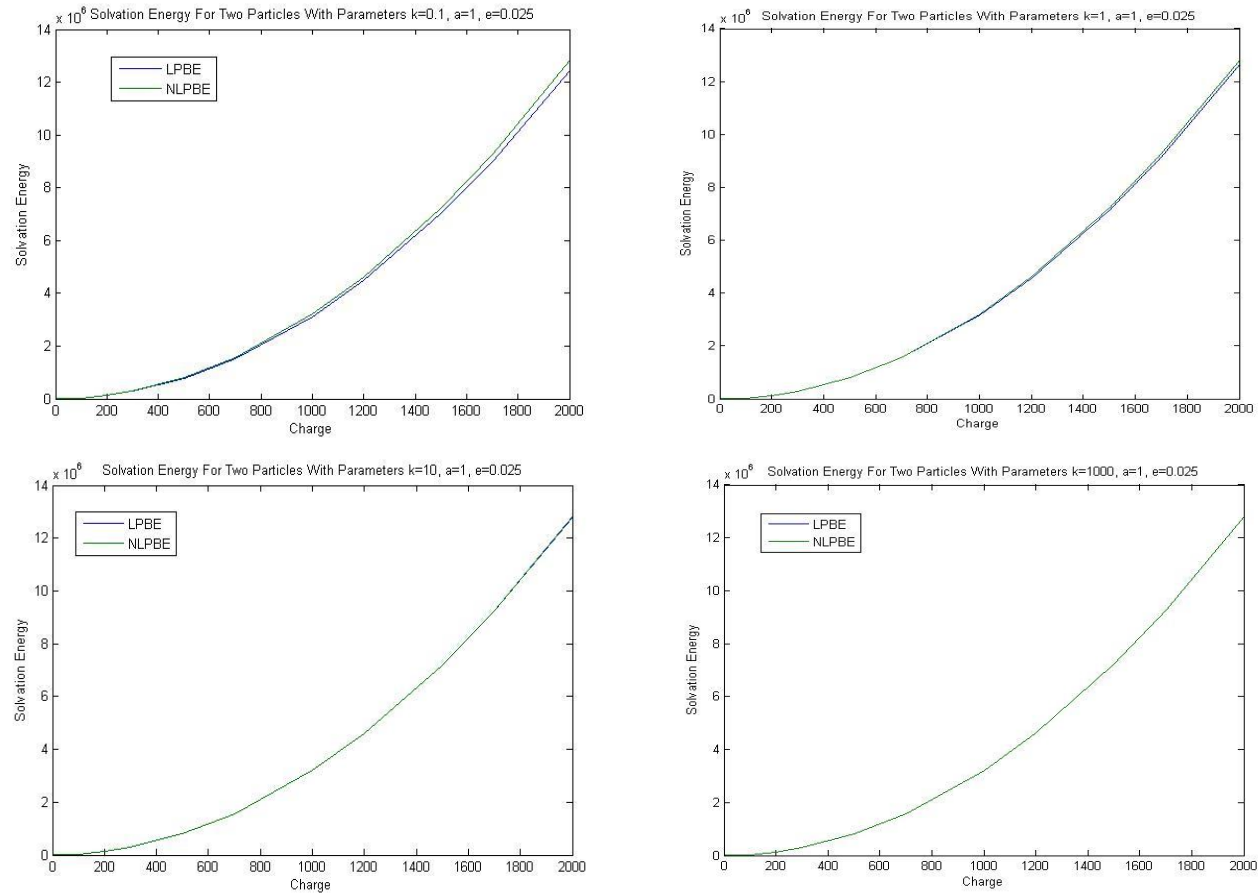
Figure 32: Solvation Energy for Two Particles with Parameters a=1 and ε=0.025. $\bar{k}$ Varies Clockwise from 0.1 to 1 to

10 to 1000

The previous results were characterized by a dielectric mismatch between the particle and the solution space. In the following results, the dielectric mismatch will be removed and ε will be equal to one.

In the case where $\bar{k}$=0.1 $\frac{1}{\AA}$ and a varies, notice that the linear PBE computes a negative solvation energy. The convention used implies that the two particles increase the relative energy of the system. For a=0.1$\dot{A}$, one can see that the solvation energy is -1e5 J at a charge of 2000C. For a=0.5$\dot{A}$, the solvation energy increase to approximately -7e4J and for a=1$\dot{A}$, the solvation energy approaches -5e4J and finally when a=2$\dot{A}$, the energy is computed to be -2.5 e4J. Thus, the solvation energy increases as the distance between particles increases and the particles would experience a slower dissolving process. Note that the nonlinear PBE is given by 3.2e5J. Also, note that for small charges, the linear and nonlinear PBE approximate similar solutions and the results diverge as the charge increases.

The same trend can be seen for $\bar{k}$=1$\frac{1}{\AA}$. However, both the linear and nonlinear PBE compute positive solvation energy. For a=0.1$\dot{A}$, the solvation energy is calculated to be 1.2e5J. For a=0.5$\dot{A}$, the solvation energy is approximately 1.4e5J. It increases to 1.5e5J for a=1$\dot{A}$ and reaches nearly 1.55e5J for a=2$\dot{A}$. As discussed above, when the Debye length is large and the dielectric

mismatch is small, a relatively large portion of the solvation energy comes from $\bar{k}$.

The gap between the results of the linear and nonlinear PBE continues to decrease as $\bar{k}$ increases. for $\bar{k}=10\frac{1}{\overset{\circ}{A}}$ and a=0.1$\overset{\circ}{A}$, the solvation energy is approximately 2.9e5J. This value stays nearly constant as a increases unlike the previous two cases when $\bar{k}$ was very small. Ultimately, when $\bar{k}$ is very large, i.e. $1000\frac{1}{\overset{\circ}{A}}$, there is no foreseeable difference between the LPBE and NLPBE results. The solvation energy is measured at 3.2e5J even as a increases.

In the case of k=$1000\frac{1}{\overset{\circ}{A}}$, the Debye length is 0.001$\overset{\circ}{A}$. This is smaller than the smallest a used, which is 0.1$\overset{\circ}{A}$. This explains why a no longer makes a difference in the solution of the solvation energy, as it is already too large compared to the Debye length.
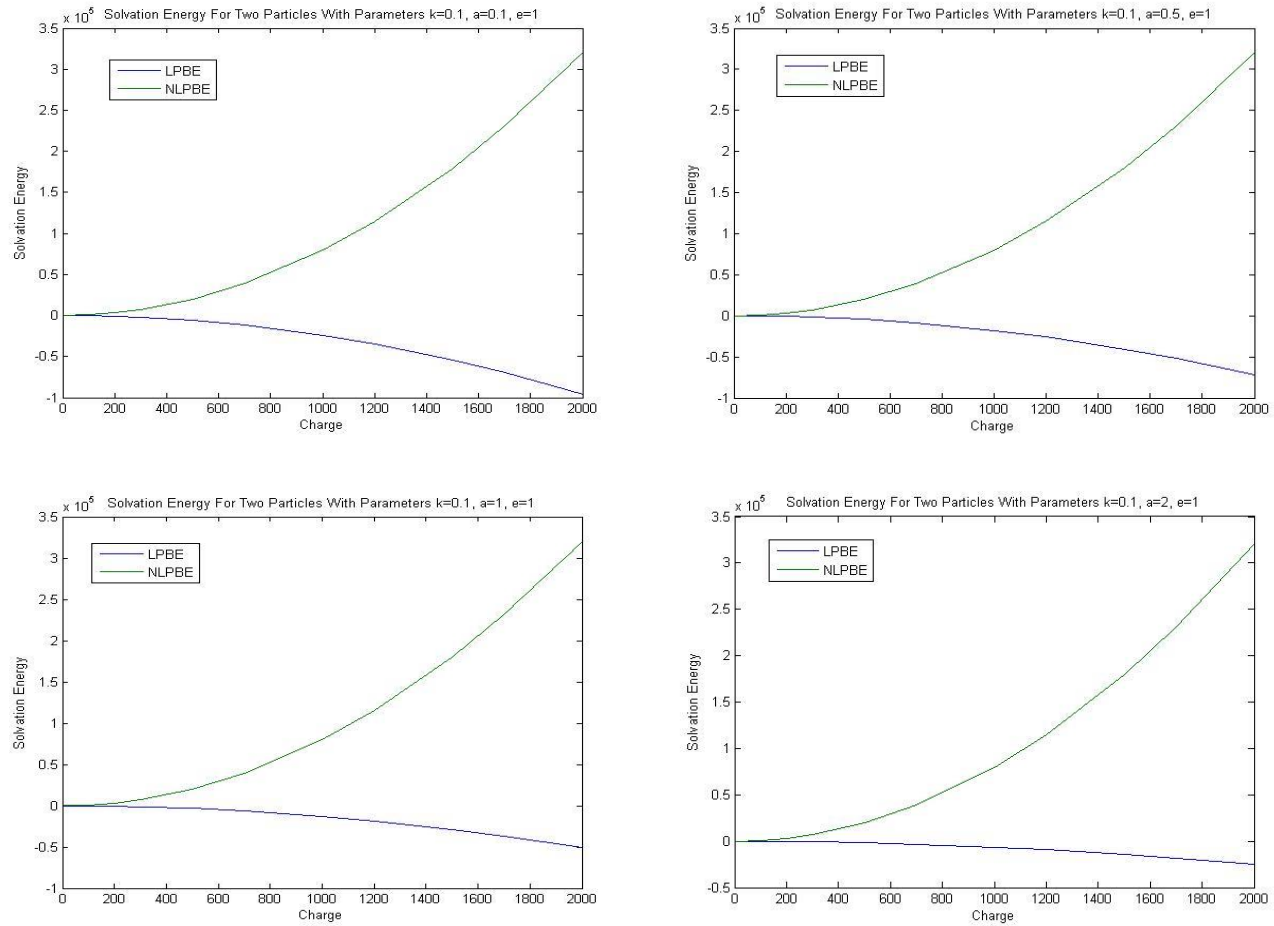
Figure 33: Solvation Energy for Two Particles with Parameters: $\bar{k}$=0.1, ε=1 and a Varies Clockwise: 0.1, 0.5, 1, 2
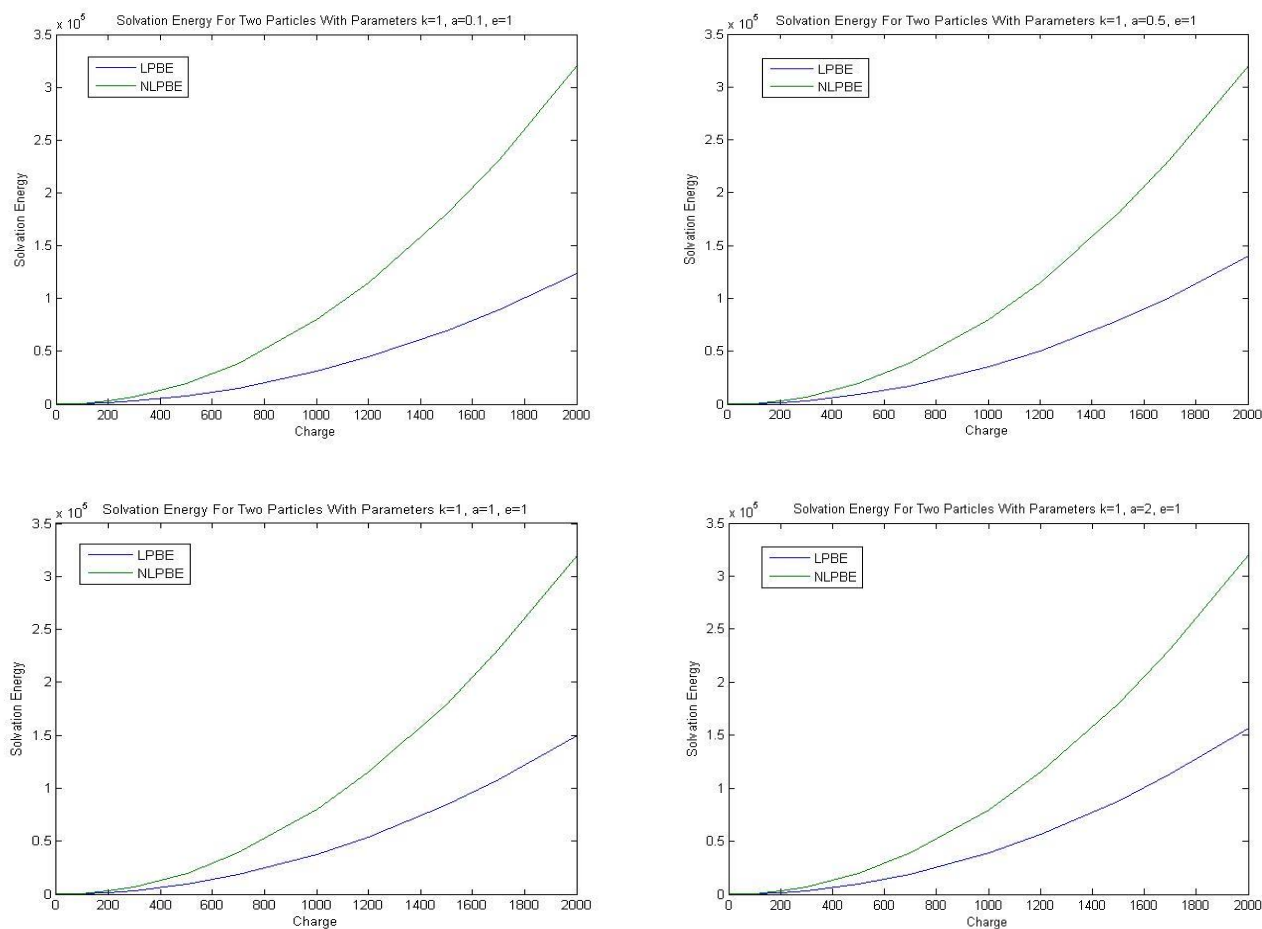
Figure 34: Solvation Energy for Two Particles with Parameters: $\bar{k}$=1, ε=1 and a Varies Clockwise: 0.1, 0.5, 1, 2
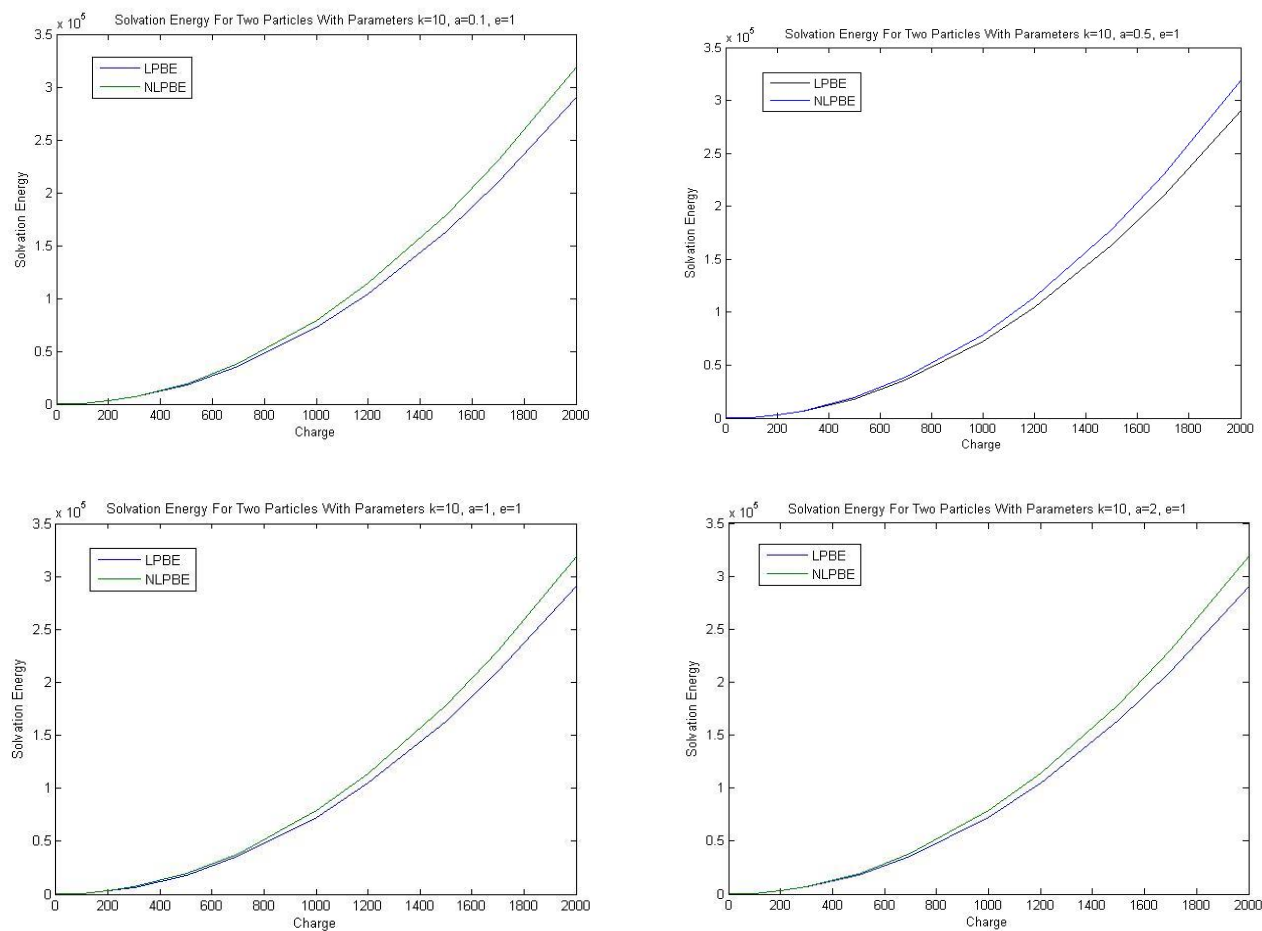
Figure 35: Solvation Energy for Two Particles with Parameters $\overline{k}$=10 and ε=1. a Varies Clockwise: 0.1, 0.5, 1 ,2
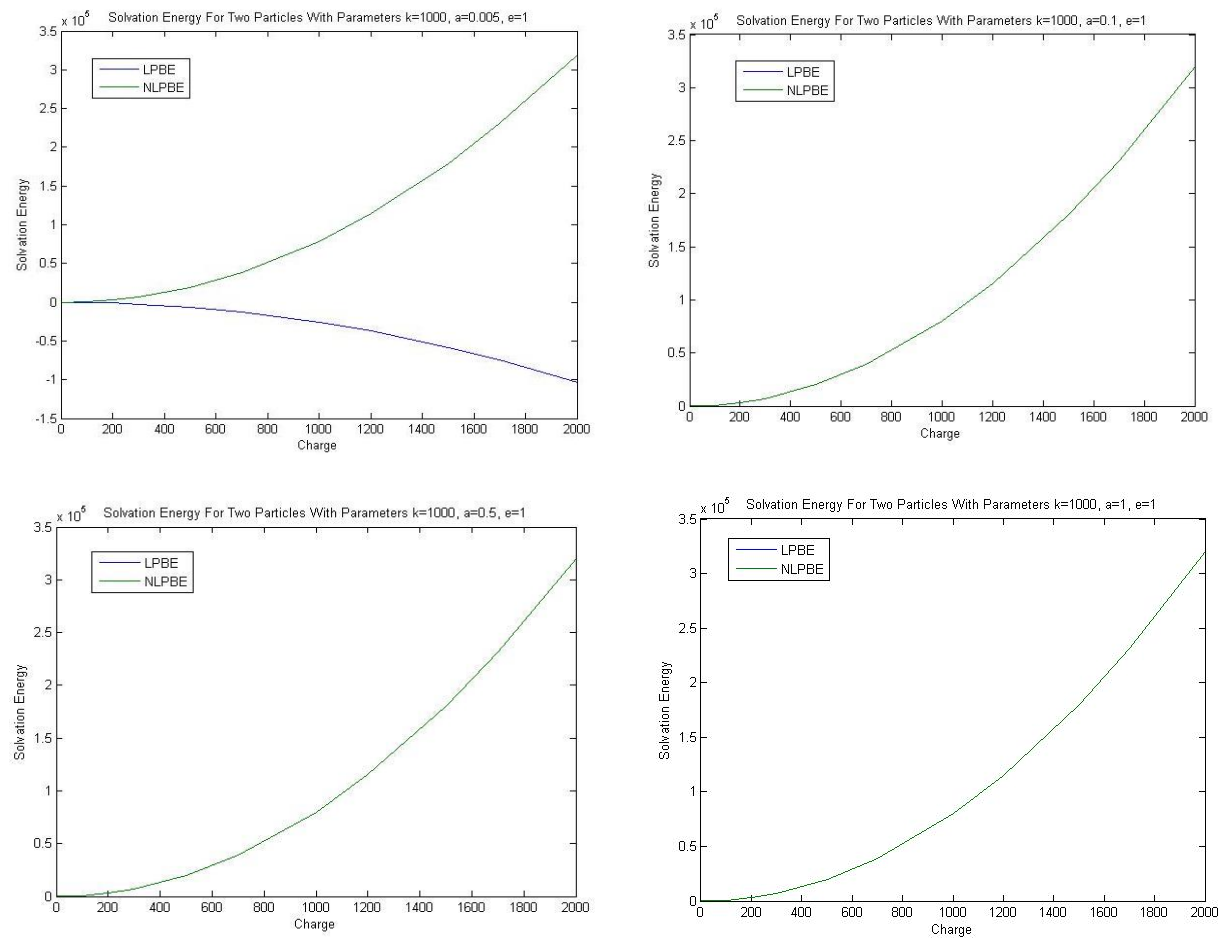
Figure 36: Solvation Energy for Two Particles with Parameters $\bar{k}$=1000 and ε=1. a Varies Clockwise: 0.005, 0.1, 0.5, 1

The effect of ε on the solvation energy can be seen in figure 37. When a high dielectric mismatch is present with a dielectric ratio of 0.025, the linear and nonlinear PBE describe a similar behavior of the solvation energy with a maximum value of 12e6 J. When the dielectric mismatch is removed and the dielectric constant of the particle is equal to that of the solvent, the LPBE and NLPBE achieve slightly different maximum magnitudes for the solvation energy. As expected the NLPBE predicts a higher value of 3.1e5, while the LPBE predicts a value of approximately 2.9e5 J. Thus, the dielectric ratio is inversely proportional the solvation energy.
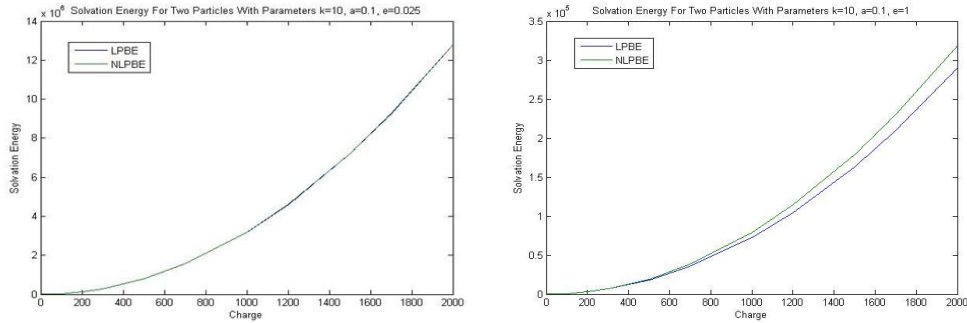
Figure 37: Effect of e on the Solvation Energy For $\bar{k}$=10 and a=0.1. The left plot has ε=0.025 while the image on the right experiences no dielectric mismatch

3.3.2 Interaction Energy

The interaction energy between the two particles is defined as the solvation energy from the two particles minus twice the solvation energy from one particle. The interaction energy from all the cases above was calculated and plotted below. Table 5 shows the parameters used.

Let's first examine the set of results for a high dielectric mismatch and ε=0.025. The dielectric ratio will stay constant throughout. The first four plots will show the results of the interaction energy between two particles for a Debye length of one as the distance and the charge between them increase. One can see that there is no interaction energy using the nonlinear model. The linear model shows an exponential decrease in interaction energy until it reaches a maximum of -4.5e4J at Q=2000C. As $\bar{k}$ and ε stay constant by a increases to $2\dot{A}$, the linear and the nonlinear model begin to agree. The interaction energy increases exponentially from zero to a maximum of 12.2e5J.

When $\bar{k}$ increases to $10\frac{1}{\dot{A}}$ and even $1000\frac{1}{\dot{A}}$, the models for ε=0.025 and a varying from $0.5\dot{A}$ to $2\dot{A}$ do not change. Only when a=$0.1\dot{A}$ can one see a disparity between the linear and nonlinear models. When the Debye length equals the distance between the two particles, the nonlinear model calculates a maximum interaction energy of 10J, while the linear model decreases exponentially to about -510J at Q=2000C.

Consider the case when $\bar{k}=1000\frac{1}{\mathring{A}}$ and $a=0.1\mathring{A}$, one can see a continuous increase of the interaction energy. The nonlinear PBE model predicts a maximum interaction energy of 1300J, while the linear PBE model shows no interaction energy between the particles. This is the complete opposite of the case where the Debye length was equal to $1\mathring{A}$. In the latter, the NLPBE model initially showed no interaction energy between the particles, while the linear model predicted a large negative interaction energy.
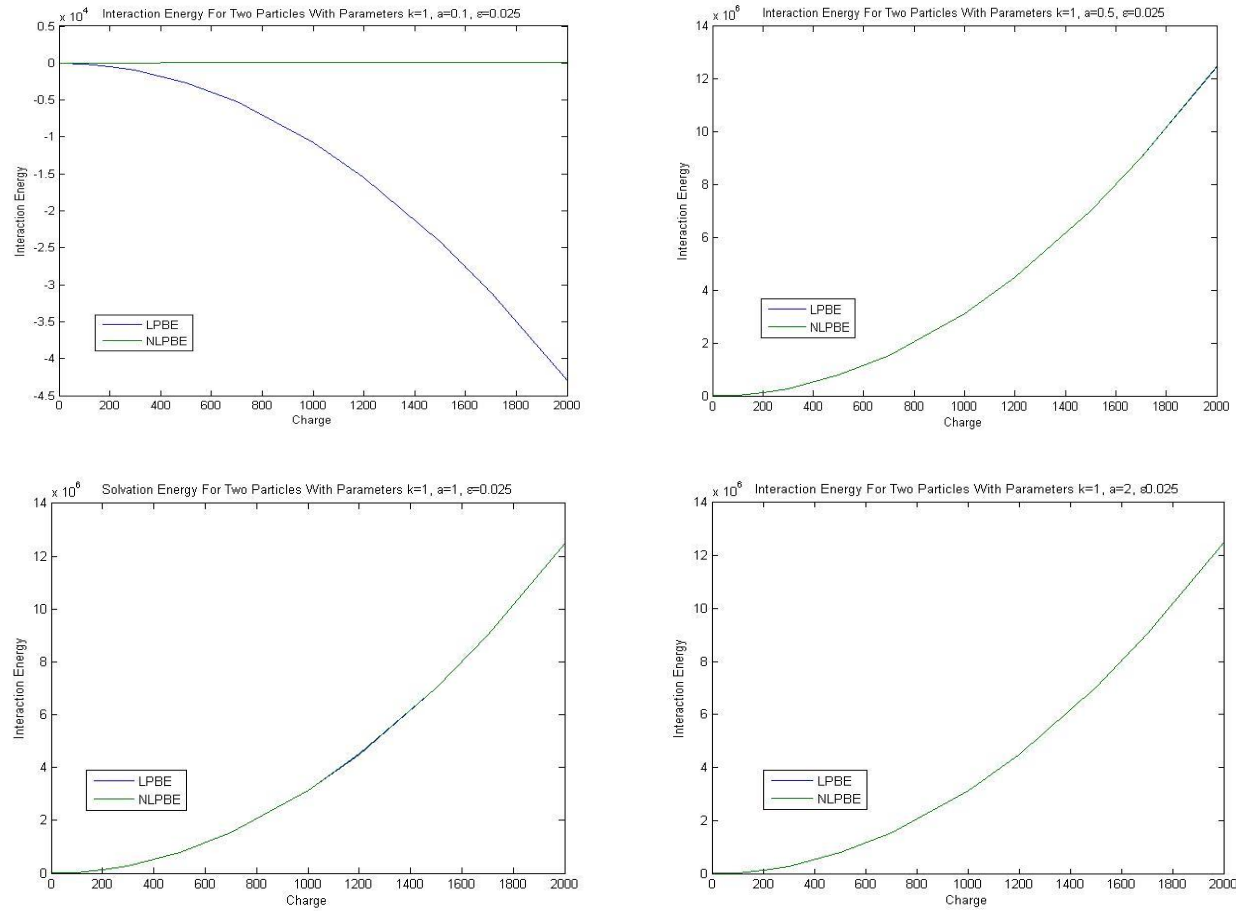
Figure 38: Interaction Energy of Two Particles with Parameters $\bar{k}$=1 and ε=0.025. a varies respectively: 0.1, 0.5 ,1, 2
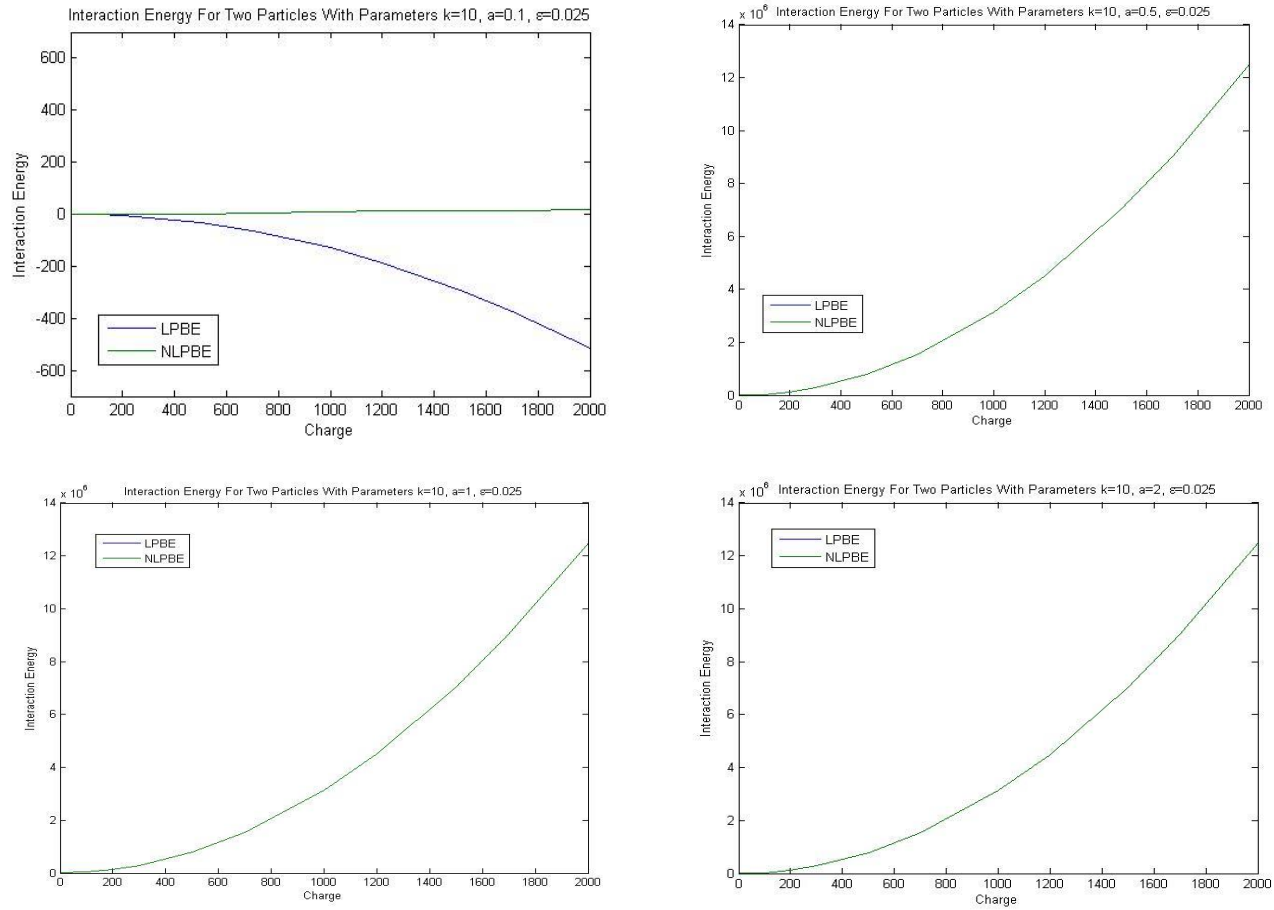
Figure 39: Interaction Energy of Two Particles with Parameters $\overline{k}$=10 and ε=0.025. a varies respectively: 0.1, 0.5, 1, 2

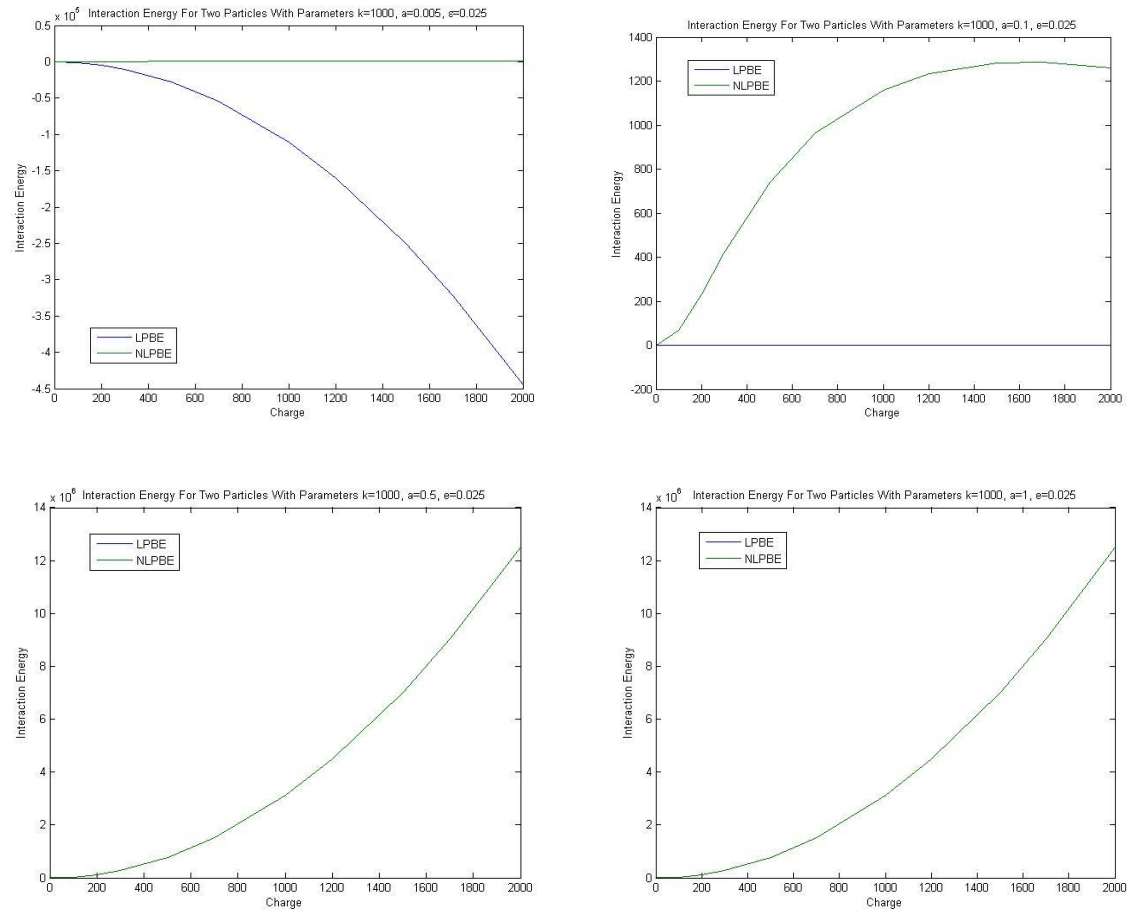Figure 40: Interaction Energy of Two Particles for $\bar{k}$=1000 and ε=0.025. a varies from 0.005, 0.1, 0.5 to 1 respectively

Consider a setting with no dielectric mismatch. The Debye length will have considerably more influence on the interaction energy as can be seen from the following plots.

For a Debye length of one, as $\bar{k}$ stays constant and a increases, the nonlinear PBE model predicts that the interaction energy between the two particles will remain zero even as Q increases to 2000C. In contrast, the linear PBE model predicts a positive correlation between a and the interaction energy. When a is equal to $0.1\dot{A}$, the interaction energy is calculated to be -3.5e4J. As a increases to $0.5\dot{A}$, the solvation energy becomes -19000J. When the distance between the two spheres is equal to the Debye length, the solvation energy continues its exponential increase to almost half the value of a=$0.5\dot{A}$. Finally, when a=$2\dot{A}$, the interaction energy is approximately 2.7e3J, a factor of more than ten of the solution for a=$0.1\dot{A}$.

Let's consider the environment where $\bar{k}$=$10\frac{1}{\dot{A}}$. The nonlinear PBE demonstrates that no interaction energy exists between the two particles for a=$0.1\dot{A}$ to a=$2\dot{A}$. This may be due to the screening effect of the NLPBE. The solution to the LPBE decreases exponentially from zero to a minimum value at Q=2000C. For a=$0.1\dot{A}$, the value of the solvation energy is -480J and by the time a becomes $2\dot{A}$, the maximum value of the solvation energy agrees with the NLPBE model. Finally for $\bar{k}$=$1000\frac{1}{\dot{A}}$, for a =$0.005\dot{A}$, the LPBE predicts the

presence of a high interaction energy between the particles, whereas the NLPBE

predicts that no interaction energy exists. As a increases to $0.1\dot{A}$ and reaches $1\dot{A}$,

both the LPBE and the NLPBE predict that there is no interaction energy between
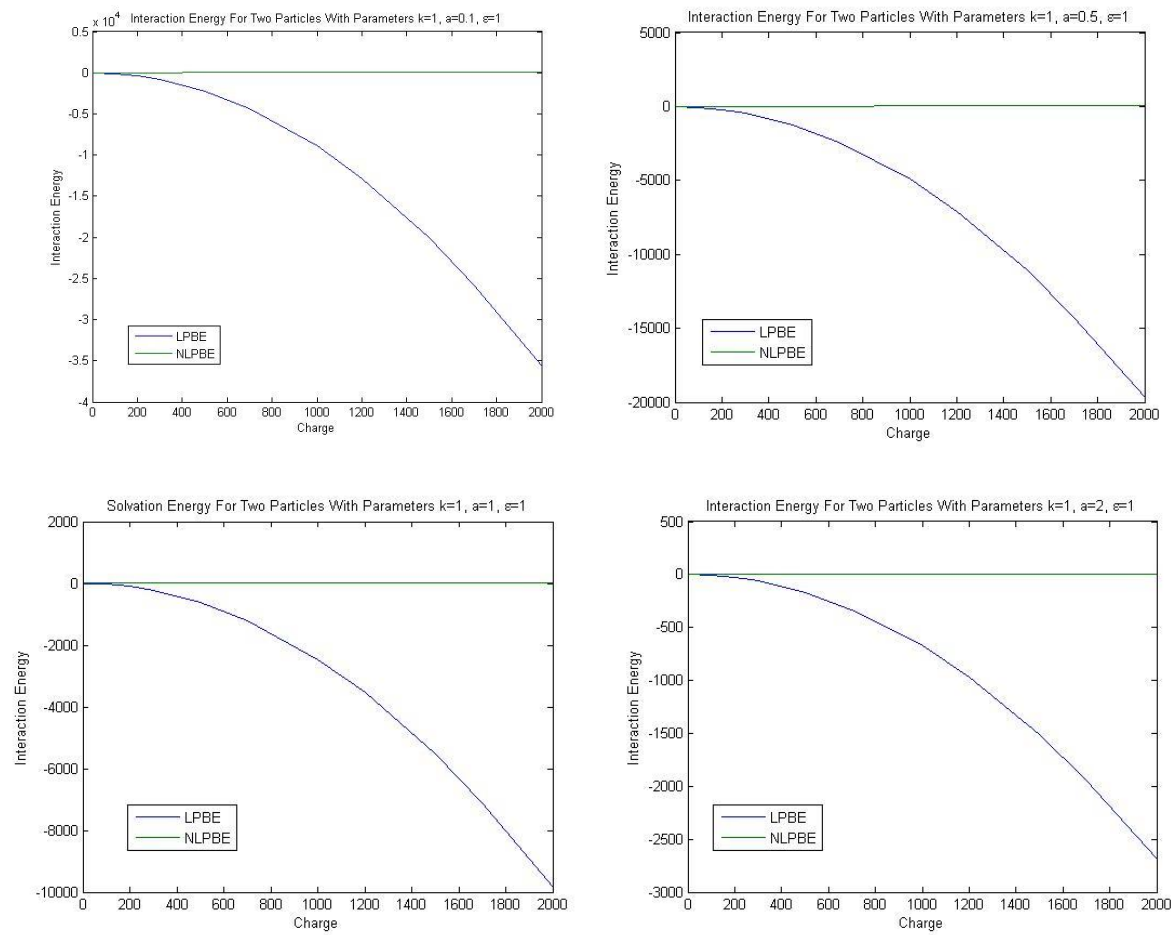
the two particles.

Figure 41: The Interaction Energy of Two Particles with Parameters $\bar{k}$=1 and ε=1. a varies clockwise from 0.1 to 2
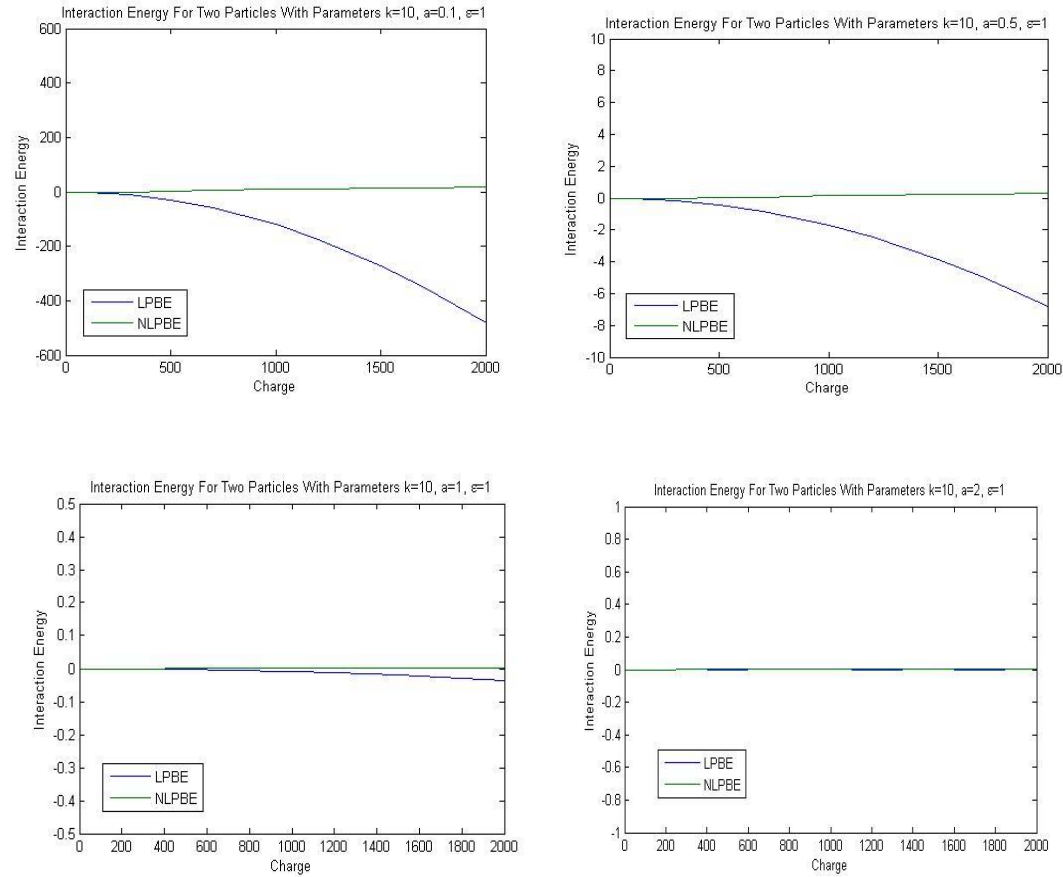
Figure 42: The Interaction Energy of Two Particles with Parameters $\overline{k}$=10 and ε=1. a varies clockwise from 0.1 to 2
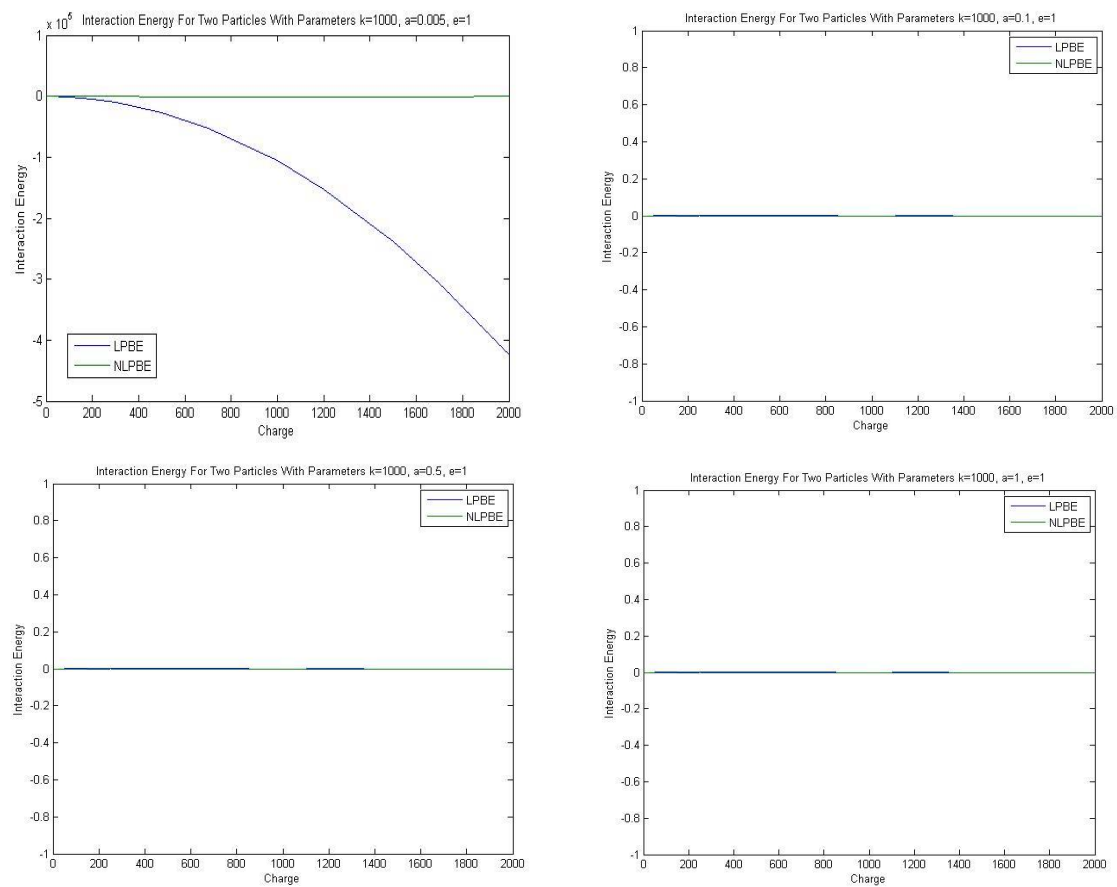
Figure 43: The Interaction Energy of Two Particles with Parameters $\bar{k}$=1000 and ε=1. a varies clockwise from 0.1 to 1

For a=0.1$\dot{A}$ and ε=1, three $\bar{k}$ values, ranging from $1\frac{1}{\dot{A}}$ to $1000\frac{1}{\dot{A}}$ were

chosen to demonstrate the effect of the Debye length on the interaction energy. In

all cases, the non-linear PBE predicts no interaction energy between the two

particles. The LPBE, however, determines that there is an interaction energy

present between the two particles with Debye lengths of $1\dot{A}$ and $0.1\dot{A}$, of -20000J

and -7J respectively. When $\bar{k}$=$1000\frac{1}{\dot{A}}$, the LPBE finds no interaction energy.
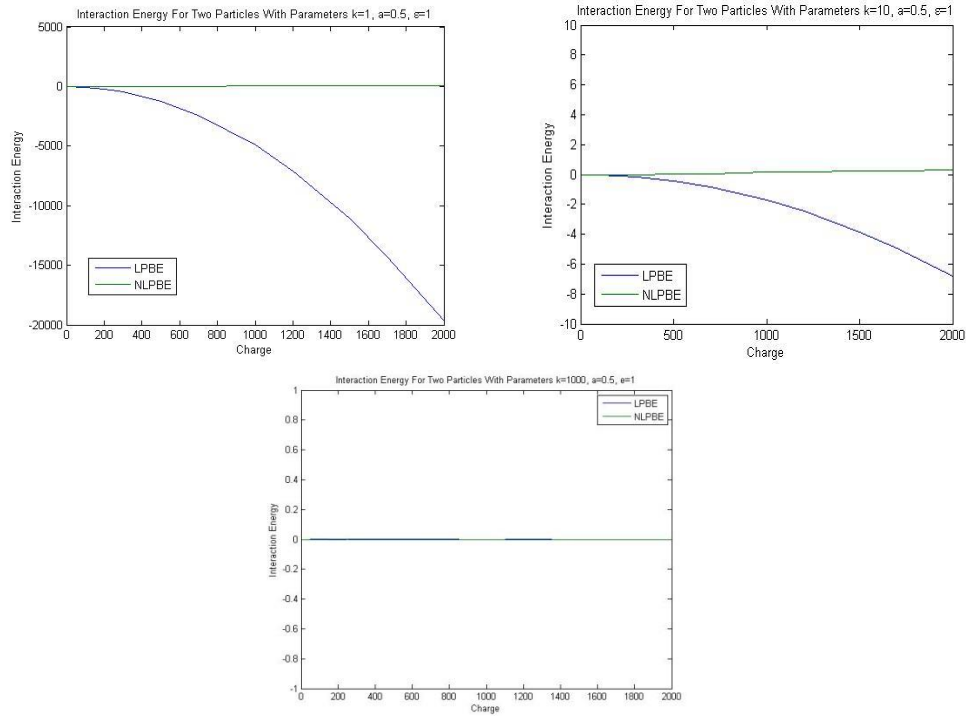
Figure 44: The Effect of $\bar{k}$ on the Interaction Energy for a=0.1 and ε=1. $\bar{k}$ varies

from 0.1 to 1 to 1000

Next, let's examine the effect of ε on the interaction energy for a Debye length of $0.1\dot{A}$. For $a = 0.1\dot{A}$, the NLPBE predicts no interaction energy between the particles, while the LPBE calculates an interaction energy of -510J for $\varepsilon = 0.025$ and -480J for $\varepsilon = 1$. When a is increased to $0.5\dot{A}$, the high dielectric mismatch creates a large interaction energy between the two particles of approximately 12e6J. Removing the dielectric mismatch leads to a very small interaction energy of -7J as calculated by the LPBE and none as predicted by the NLPBE.
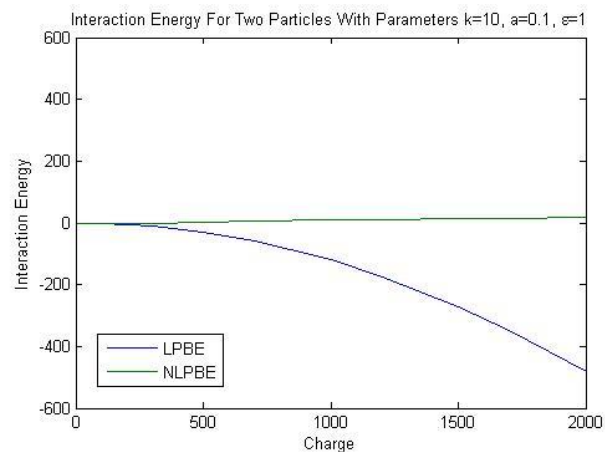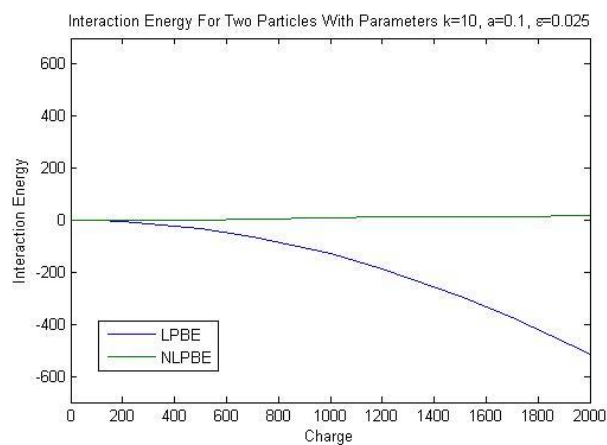
Figure 45: The Interaction Energy of Two Particles With Parameters $\overline{k}$=10 and a=0.1. The Left Image Has a Dielectric

Ratio of 0.025, While the Right Image Does Not Experience a Dielectric Mismatch

Figure 46: The Interaction Energy of Two Particles With Parameters $\bar{k}$ =10 and a=0.5. The Left Image Has a Dielectric

Ratio of 0.025, While the Right Image Does Not Experience a Dielectric Mismatch

3.3.3 Potential field surface and contour plots

In this section, six cases will be used to ascertain the effects of ε, a, $\bar{k}$ and Q on the potential field. The surface and contours of the potential will be plotted and described for each case. The table below contains the parameters used.
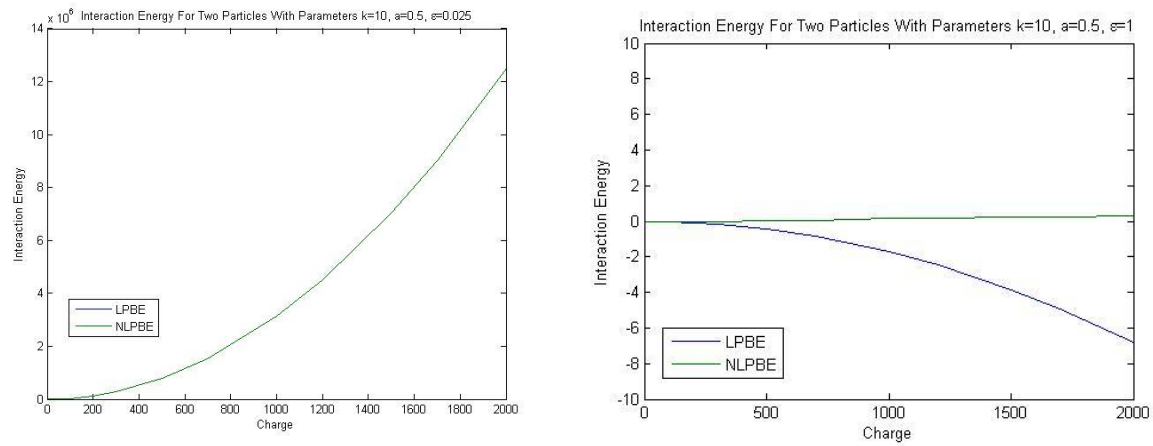
Table 6: Parameters Used to Study the Surface Potential

Case Number	$\bar{k}\left(\frac{1}{\AA}\right)$	$a\left(\AA\right)$	ε	Q
1	1	2	Varies	1
2	Varies	0.1	1	300
3	1	Varies	1	2000
4	1	2	1	1500
5	10	0.1	0.025	Varies
6	10	0.1	0.025	200

In the first model, a comparison is made between two identical particles each with parameters $\bar{k}=1\frac{1}{\AA}$, $a=2\AA$ and Q=1C and a varying parameter ε. The left image reflects the use of a dielectric ratio of one while the right image contains $\varepsilon=0.025$. One can see that introducing a dielectric mismatch increases the potential significantly. For $\varepsilon=0.025$, the maximum potential is located at the center of the spheres with a magnitude of approximately 28V, while $\varepsilon=1$ only allows a maximum potential of 0.75V. Furthermore, a trough is created a distance of approximately $0.4\AA$ from the center of the sphere. Also note that some potential is present at the boundary of the sphere when the dielectric ratio is one but is nonexistent for $\varepsilon=0.025$.

Case 1:
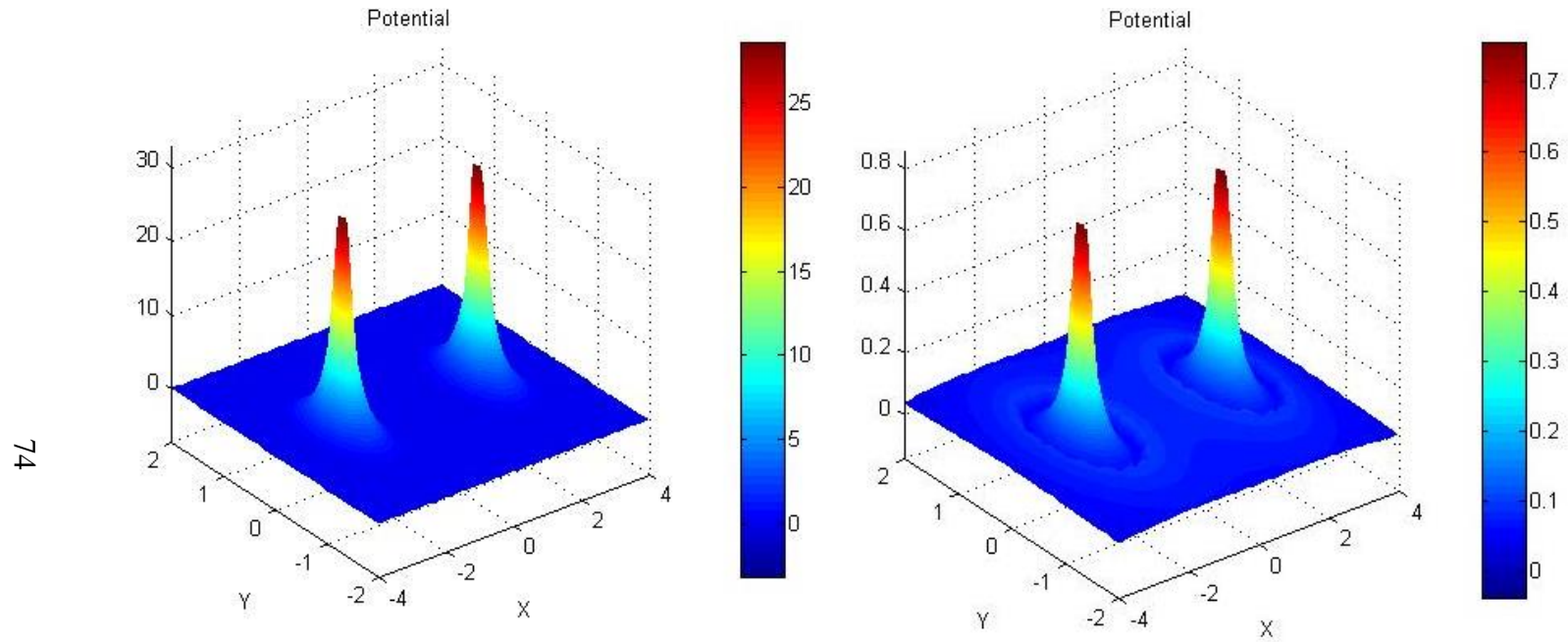
Figure 47: The Potential Field of Two Particles with Parameters: $\bar{k}=1$, $a=2$, Q=1. In the right image, $\varepsilon=1$ and $\varepsilon=0.025$ for the left image.

Figure 48: The Potential Contour Plot of Two Particles with Parameters: $\bar{k}=1$, $a=2$, Q=1. In the right image, ε=0.025

and ε=1 for the left image.

Case 2:
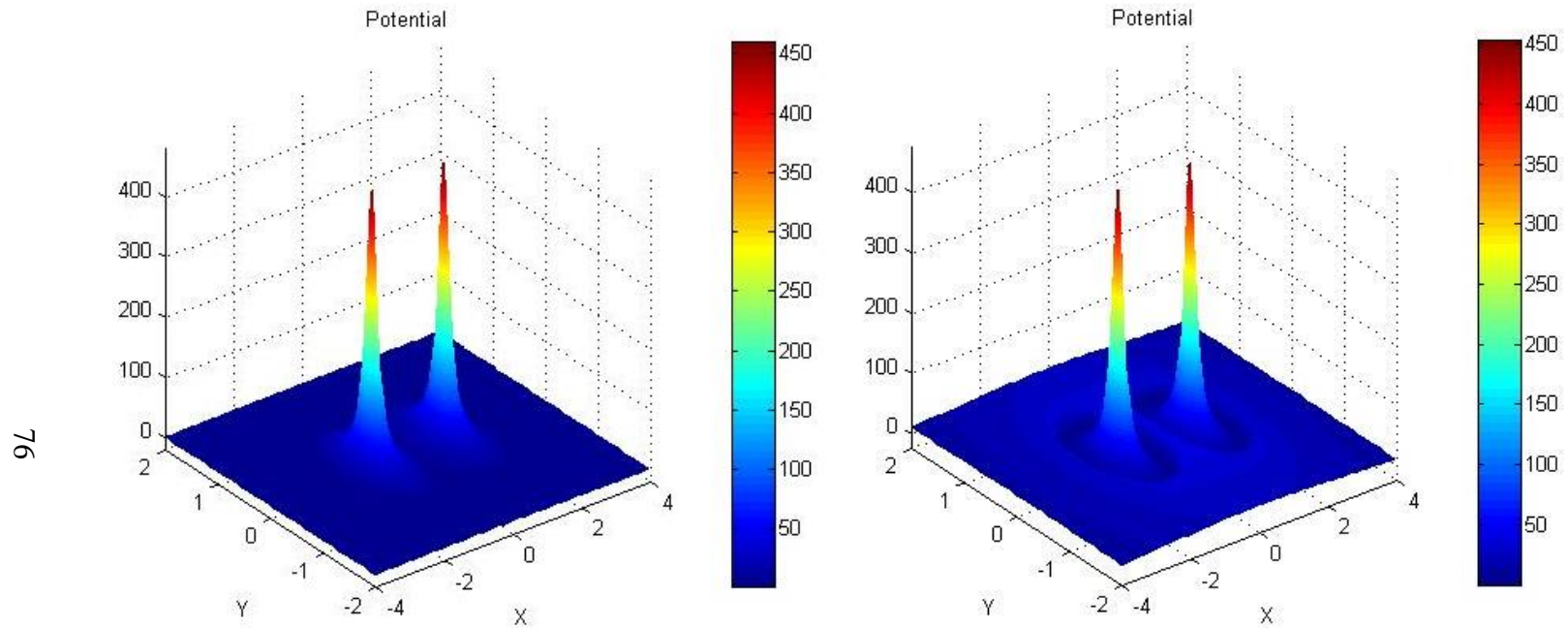
Figure 49: The Potential Field of Two Particles with Parameters: $\varepsilon=1$, $a=0.1$, Q=300. In the left image, $\bar{k}=0.1$ and

$\bar{k}=1000$ for the right image.

Figure 50: The Potential Contour Plot of Two Particles with Parameters: ε=1, a=0.1, Q=300. In the right image, $\bar{k}$=0.1

and $\bar{k}$=1000 for the left image.

In this model, the effect of the Debye length on the potential field is addressed. The two spheres are a distance $0.1\dot{A}$ apart and experience no dielectric mismatch. A relatively small charge of 300C is applied at the center of each sphere. When $\bar{k}$ is $0.1\frac{1}{\dot{A}}$, the maximum potential, located at the center of the spheres, is evaluated at 461V. Increasing $\bar{k}$ to $1000\frac{1}{\dot{A}}$ yields a maximum potential of 453V. Thus, a large increase of $\bar{k}$ when the charge applied is small, leads to a rather insignificant decrease in the potential. However, a small potential is generated between the two spheres when $\bar{k}$ is large that is not present when $\bar{k}$ is small.

Case 3:
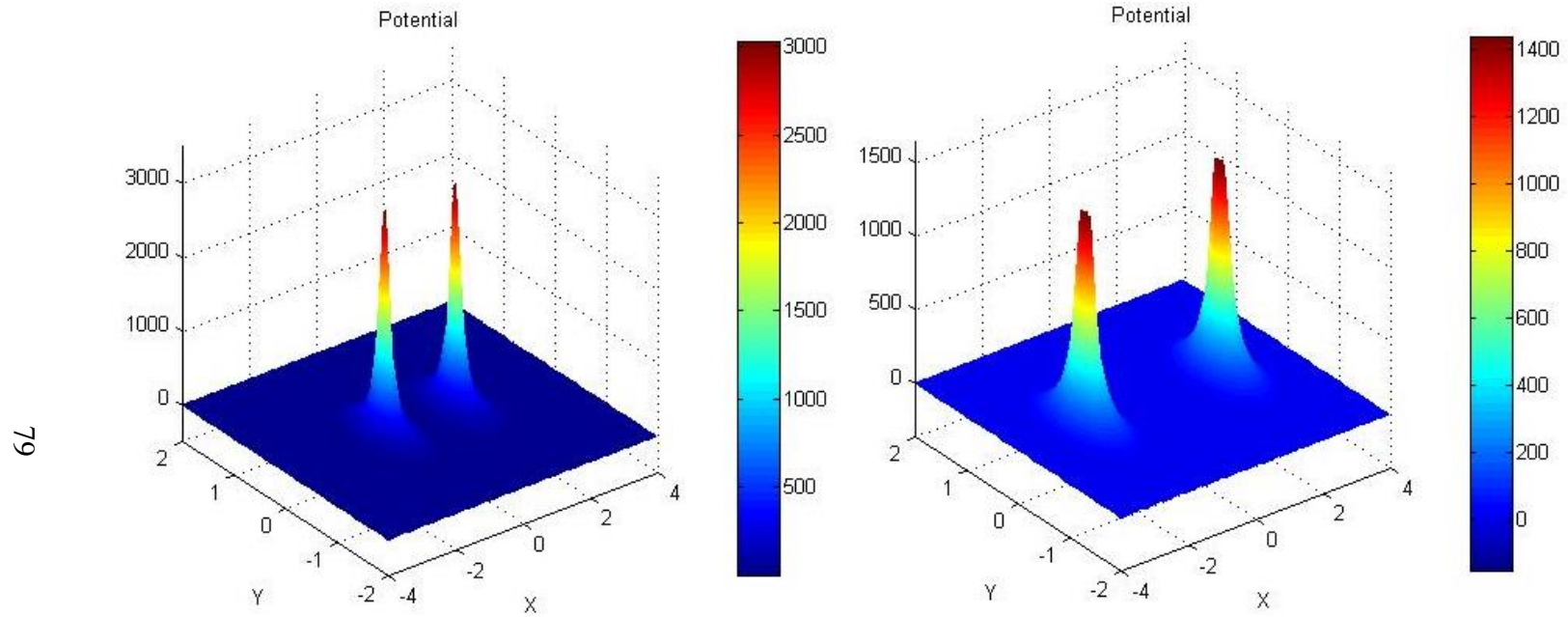
Figure 51: The Potential Field of Two Particles with Parameters: $\bar{k}=1$, $\varepsilon=1$, $Q=2000$. In the left image, $a=0.1$ and $a=2$

for the right image.
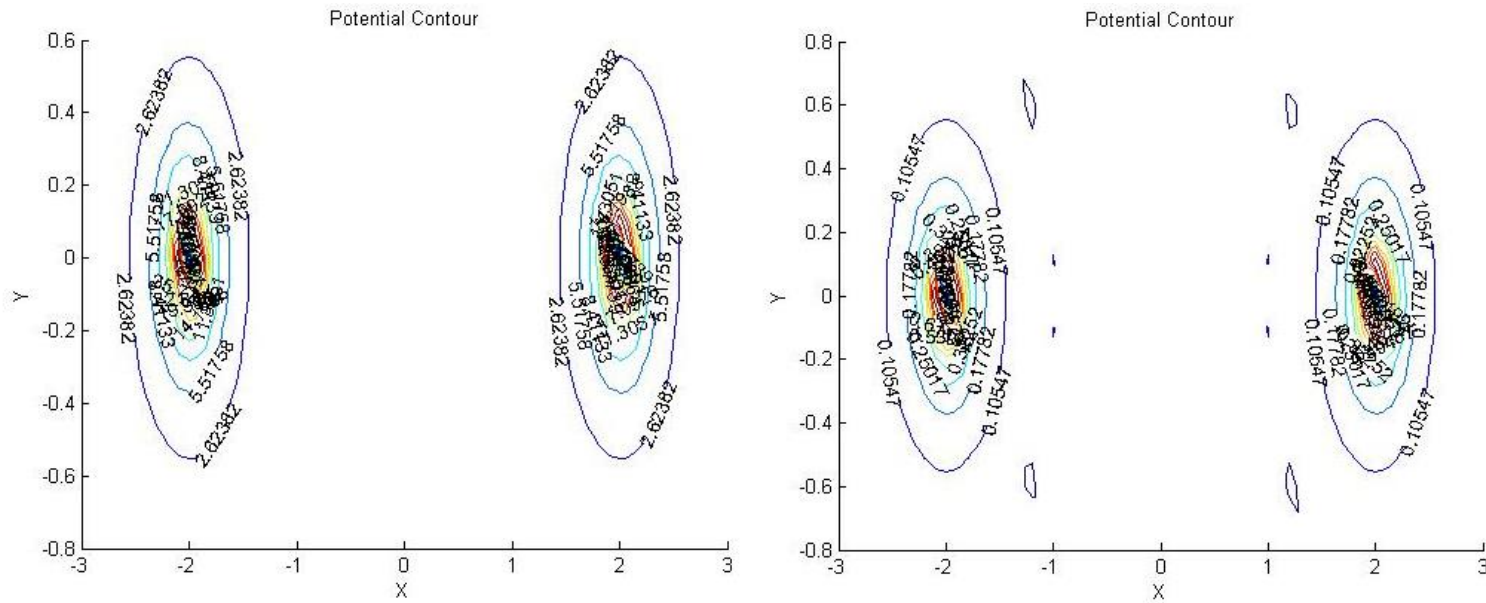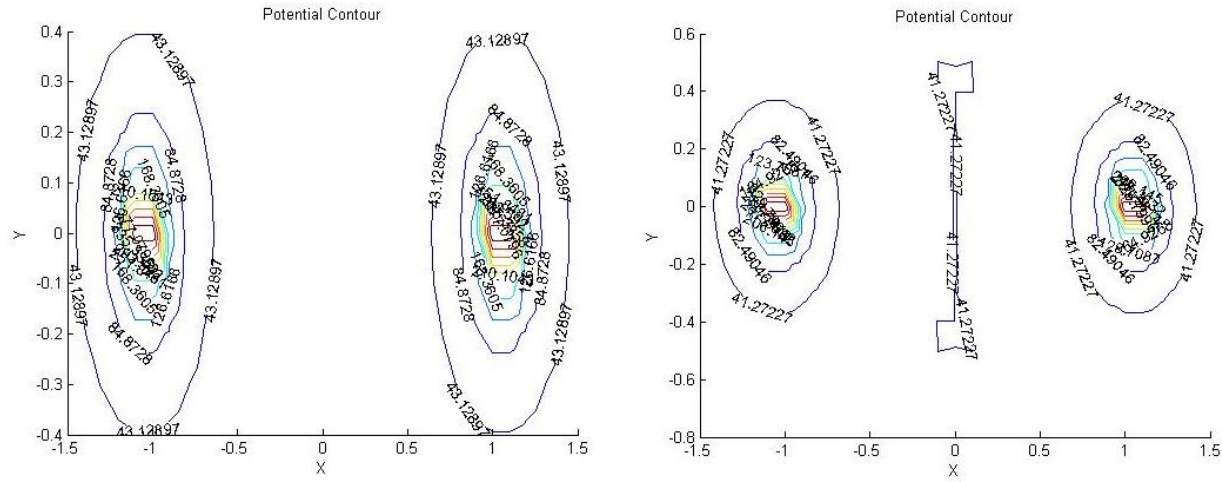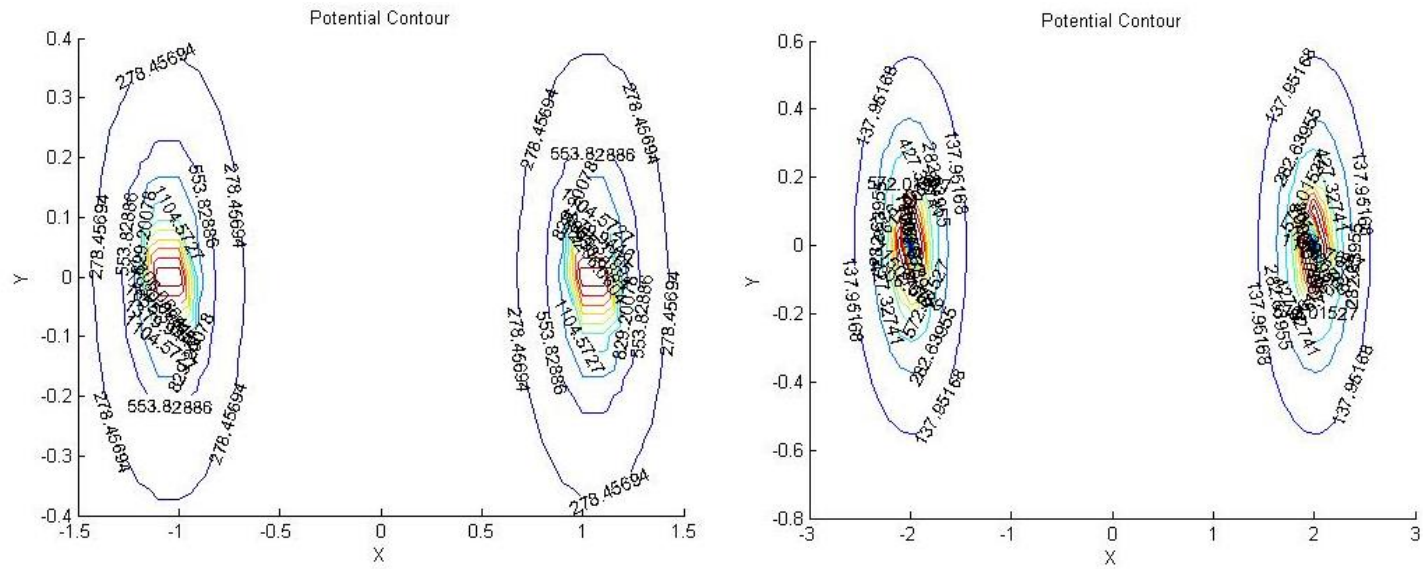
Figure 52: The Potential Contour Plot of Two Particles with Parameters: $\bar{k}$=1, ε=1, Q=2000. In the right image, a=0.1

and a=2 for the left image.

This example demonstrates the effect of the distance between the two particles on the potential field. Let the two particles be a distance $0.1\mathring{A}$ from each other, it can be shown that the maximum potential, located at the center of the spheres reaches a magnitude of 3000V. It decreases as the distance from the center of the spheres increases. When the two particles are separated by $2\mathring{A}$, the maximum potential decreases to 1400V.

Case 4:

Figure 53: The Potential Field of Two Particles with Parameters: $\bar{k}$=1, a=2, ε=1 and Q=1500. The Left Image Displays

the Potential Field Calculated by the LPBE, While the Right Image Shows the Potential Field of the NLPBE.
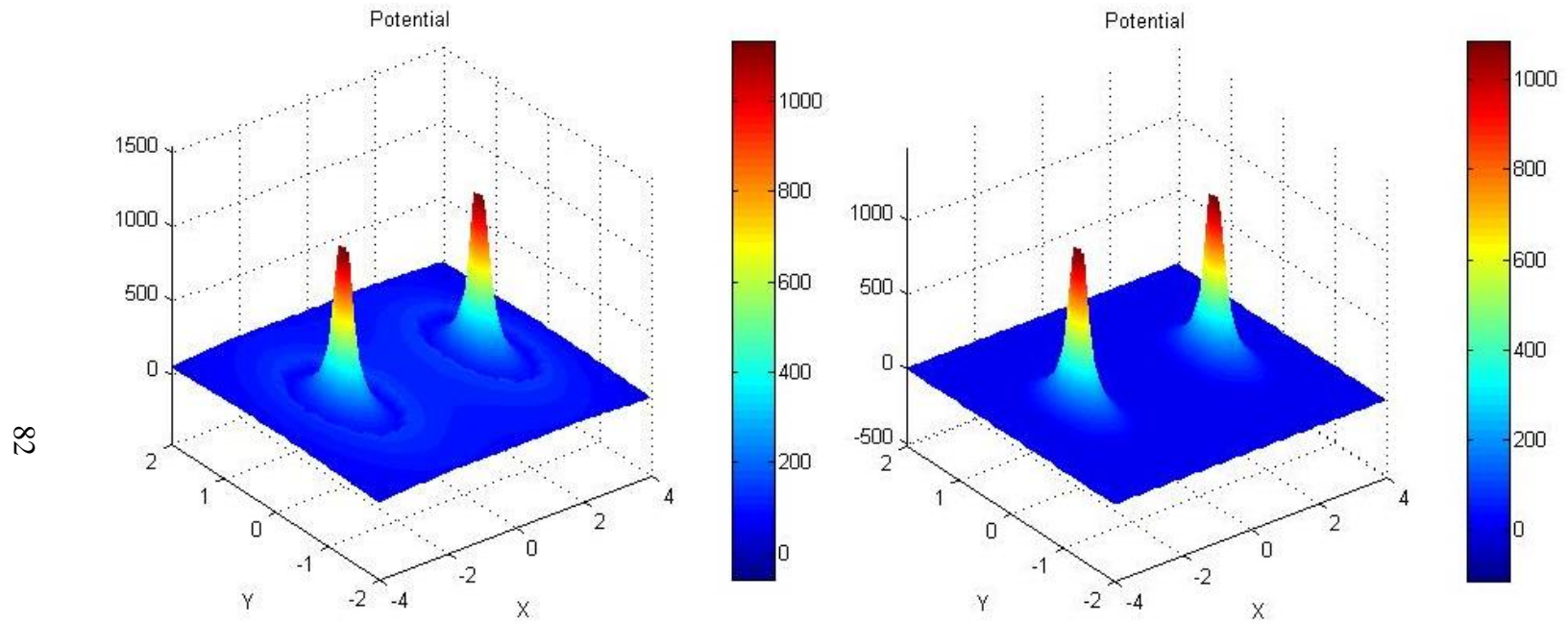
Figure 54: The Potential Contour Plot of Two Particles with Parameters: $\bar{k}=1$, $a=2$, $\varepsilon=1$ and Q=1500. The Left Image

Displays the Potential Field Calculated by the LPBE, While the Right Image Shows the Potential Field of the NLPBE.

Case four allows for a comparison between the LPBE and NLPBE. Two spheres with parameters $\bar{k}=1$, $a=2$ and $\varepsilon=1$ experience a charge of 1500C each. The potential surface and contours for the LPBE and NLPBE are plotted. It is evident from the plots above that the LPBE predicts a higher maximum potential by approximately 8%. The LPBE also shows some potential along the boundary of the spheres and a crater like dip a distance 0.3 $\dot{A}$ from the center of the spheres unlike the NLPBE which shows a smooth contour.

Figures 51 and 52 display the difference in the potential when the charge is increased and all other parameters remain unchanged. The two identical spheres have parameters $\bar{k}=10\frac{1}{\dot{A}}$, $a=0.1\dot{A}$ and $\varepsilon=0.025$. When a charge of 200C is applied, the maximum potential reached 12000V. It increases to 18000V when the charge is increased to 300C.

Case six is used to compare the potential obtained from one and two spheres. All spheres are identical with parameters $\bar{k}=10\frac{1}{\dot{A}}$, $a=0.1\dot{A}$, $\varepsilon=0.025$ and a charge of 200C is applied at the center of each sphere. The maximum potential attained by one sphere is 5727V. When a sphere is added a distance 0.1 $\dot{A}$ away, the maximum potential increases to 12093V. As such, the addition of particles and their interaction energies significantly alter the potential field

Case 5:
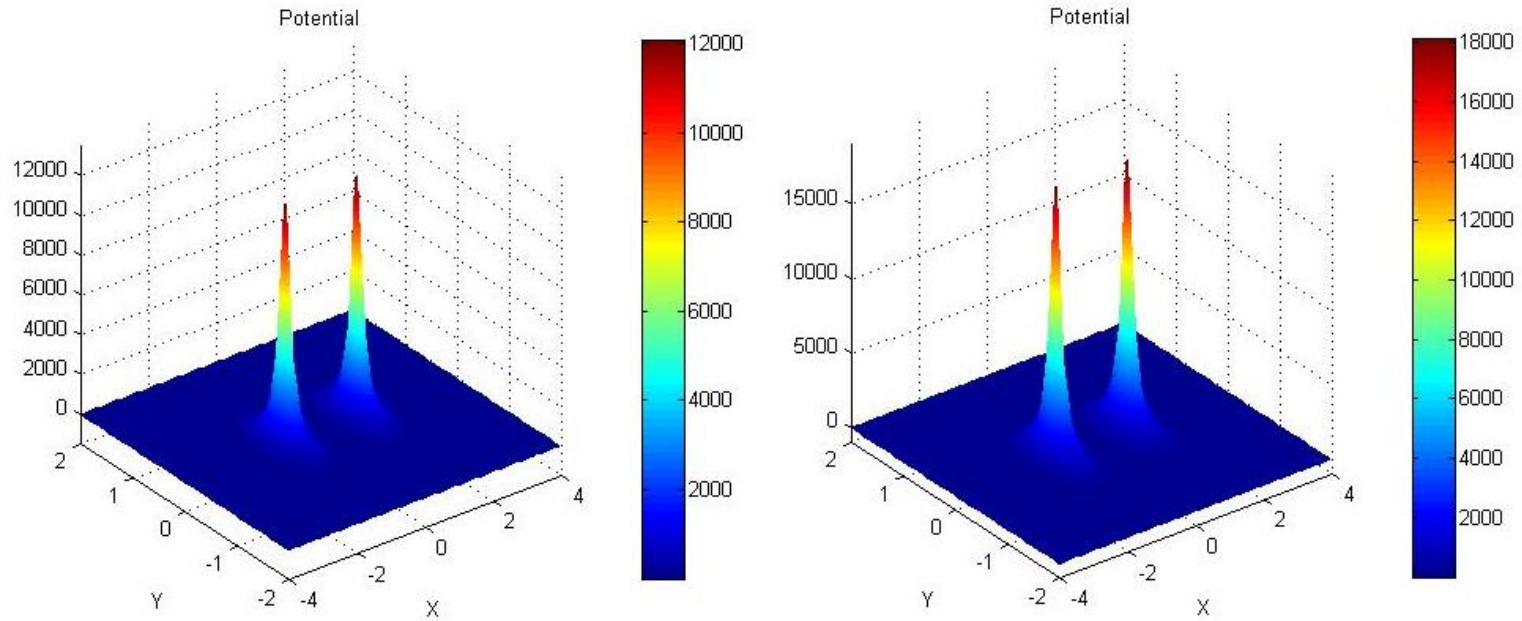
Figure 55: The Potential Field of Two Particles with Parameters: $\bar{k}$=10, a=0.1, ε=0.025. Q=200 for the Image on the

Right and 300 for the Image on the Left.

Figure 56: The Potential Contour Plot of Two Particles with Parameters: $\bar{k}$=10, a=0.1, ε=0.025. Q=200 for the Image

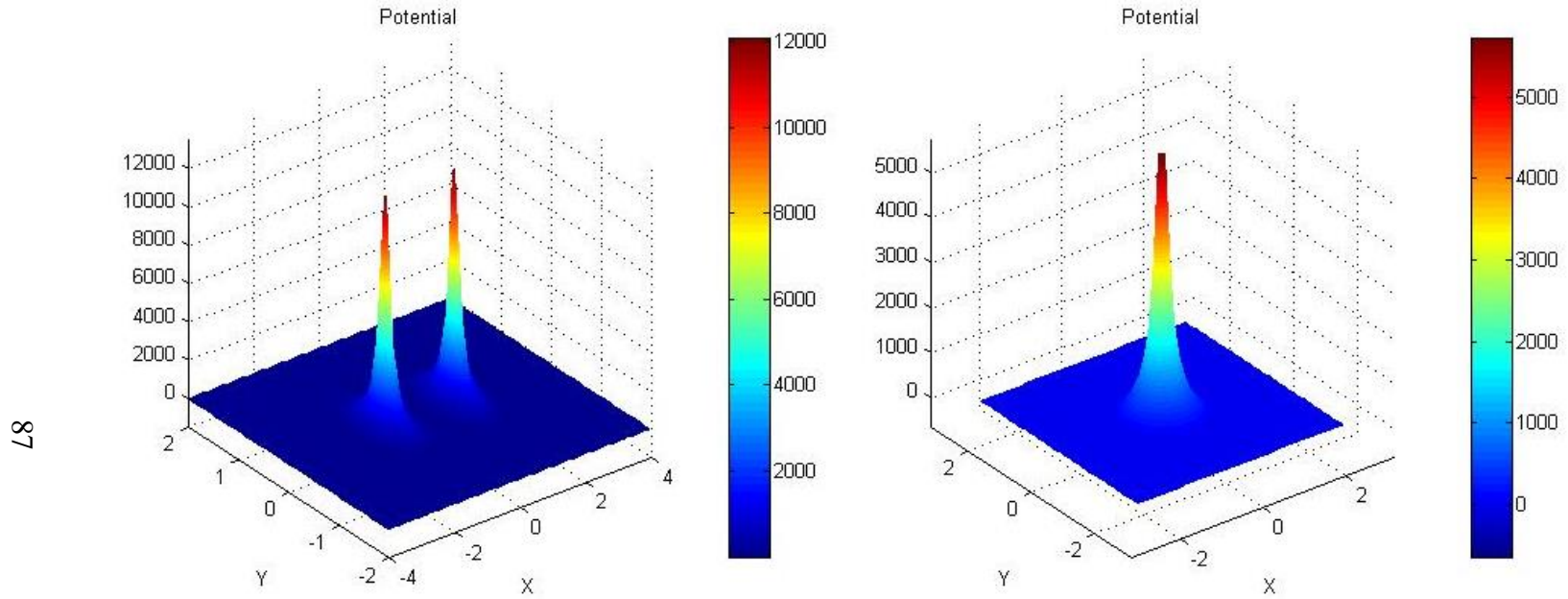on the Right and 300 for the Image on the Left.

Case 6:

Figure 57: A Comparison of the Potential Field for One and Two Particles with Parameters $\bar{k}$=10, a=0.1, ε=0.025 and
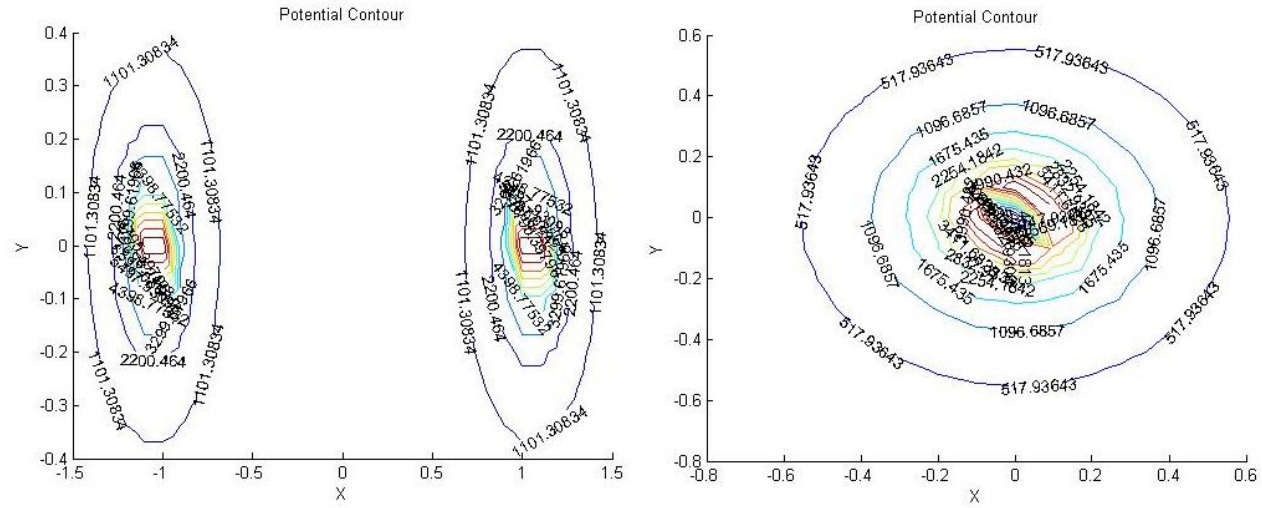
Q=200

Figure 58: A Comparison of the Potential Contour Plot for One and Two Particles with Parameters $\bar{k}$=10, a=0.1, ε=0.025 and Q=200

Chapter 4

Conclusion

A linear and a nonlinear approximation to the Poisson Boltzmann equation were applied to one and two particles in a solution using a boundary integral method. The analytical solution from Kirkwood was compared to the results of the one spherical particle, and was used to validate the code. A mesh analysis was done and a 24×24 mesh was found to be the most appropriate, meaning that it contained less than a 2% error and was relatively inexpensive computationally. The effects of $\bar{k}$ and ε on the solvation energy were examined. A high dielectric mismatch, where the dielectric ratio is less than one as in the case of biomolecules, was found to comprise a large portion of the solvation energy. As the dielectric ratio increased, the solvation energy decreased. In the case of no dielectric mismatch, the solvation energy increased as $\bar{k}$ increased. When the dielectric ratio is greater than one and $\bar{k}$ is low, the linear and nonlinear Poisson Boltzmann equations predict opposite results for the solvation energy. The maximum potential was found to be inversely proportional to ε and proportional to the applied charge.

In the case of two spheres, the effects of a, $\bar{k}$ and ε on the solvation and interaction energy were discussed. When ε and $\bar{k}$ are constant and a is less than twice the Debye length, there is significant interaction energy between the two particles. As a increases, the interaction energy decreases until it reaches 0. When

no dielectric mismatch exists and a and ε stay constant, an increase in $\bar{k}$ leads to

an increase in the interaction energy approximated by the NLPBE between the

two particles until it reaches 0. An increase in the dielectric ratio while keeping a

and $\bar{k}$ constant leads to a decrease in the interaction energy of the two particles.

With a high dielectric mismatch and ε is less than one, little difference is seen in

the interaction energy as $\bar{k}$ increases and a in invariant.

The effects of the parameters on the potential can be summed up as follows:

introducing a dielectric mismatch increases the potential significantly, a large

increase in $\bar{k}$, for a small Q, leads to a small decrease in the potential, the potential

is inversely proportional to a, the LPBE predicts a higher maximum potential than

the NLPBE and the potential is proportional to the charge applied.

References

1. Promega.com,. (2015). *Epigenetics*. Retrieved 24 April 2015, from

   https://www.promega.com/resources/product-guides-and-selectors/protocols-and-applications-guide/epigenetics/

2. 3dciencia.com,. (2012). *Fibrinogen structure | Visual science*. Retrieved 24 April 2015, from http://3dciencia.com/blog/?p=571

3. Inst.eecs.berkeley.edu,. (2015). *Protein folding*. Retrieved 24 April 2015, from

   https://inst.eecs.berkeley.edu/~ee127a/book/login/exa_protein_folding.html

4. Pang, X., & Zhou, H. (2013). Poisson-Boltzmann calculations: Van der Waals or molecular surface? Communications in Computational Physics, 13(1), 1-12.

5. Liu, Y. (2009). Fast multipole boundary element method: theory and applications in engineering. Cambridge university press.

6. Kirkwood, J. G. (1934). Theory of solutions of molecules containing widely separated charges with special application to zwitterions. The Journal of Chemical Physics, *2*(7), 351-361.

7. Zhou, H. X. (1994). Macromolecular electrostatic energy within the nonlinear Poisson–Boltzmann equation. The Journal of Chemical Physics, 100(4), 3152-3162.

8. Grochowski, P., & Trylska, J. (2008). Review: Continuum molecular electrostatics, salt effects, and counterion binding-a review of the poisson-boltzmann theory and its modifications. Biopolymers, 89(2), 93-113. Bordner, A. J., & Huber, G. A. (2003). Boundary element solution of the linear Poisson–Boltzmann equation and a multipole method for the rapid calculation of forces on macromolecules in solution. Journal of Computational Chemistry, 24(3), 353-367.

9. Lu, B., Zhou, Y., Holst, M., & McCammon, J. (2008). Recent progress in numerical methods for the poisson-boltzmann equation in biophysical applications. Communications In Computational Physics, 3(5), 973-1009.

10. Geng, W., & Krasny, R. (2013). A treecode-accelerated boundary integral poisson-boltzmann solver for electrostatics of solvated biomolecules. JOURNAL OF COMPUTATIONAL PHYSICS, 247, 62-78.

11. Koehl, P. (2006). Electrostatics calculations: Latest methodological advances. Current Opinion in Structural Biology, 16(2), 142-151.

12. Chen, J., Brooks, C. L., & Khandogin, J. (2008). Recent advances in implicit solvent-based methods for biomolecular simulations. Current Opinion in Structural Biology, 18(2), 140-148

13. Yoon, B., & Lenhoff, A. (1992). Computation of the electrostatic interaction energy between a protein and a charged surface. Journal of Physical Chemistry, 96(7), 3130-3134.

14. Zhou, H. X. (1993). Boundary element solution of macromolecular electrostatics: Interaction energy between two proteins. Biophysical Journal, 65(2), 955-963.

15. Chen, D., Chen, Z., Chen, C., Geng, W., & Wei, G. (2011). MIBPB: A software package for electrostatic analysis. Journal of Computational Chemistry, 32(4), 756-770.

16. Boschitsch, A., Fenley, M., & Zhou, H. (2002). Fast boundary element method for the linear Poisson-Boltzmann equation. Journal of Physical Chemistry B, 106(10), 2741-2754.

17. Demerdash, O., Yap, E., & Head-Gordon, T. (2014). Advanced potential energy surfaces for condensed phase simulation. (pp. 149-174). Palo Alto: Annual Reviews.

Biographical Information

The author completed her Bachelor of Science degree in mechanical engineering at the University of Houston, where she competed as a student-athlete. While there, she conducted research in computational fluid dynamics. She attended the University of Texas at Arlington for her Master of Science degree in mechanical engineering. During her studies at UTA, she conducted research under the guidance of Dr. Yang on micromolecular dynamics. The author is strongly interested in finite element analysis and plans to pursue a doctorate in the future.